Fatigue Tests of Plates and Beams With Stud Shear Connectors

J. E. STALLMEYER and W. H. MUNSE, Professors of Civil Engineering, University of Illinois, and K. A. SELBY, University of Toronto

•IN THE PAST few years there has been a great increase in the use of composite construction in both bridges and buildings. This increased use has produced some new proposals for shear connector design and more significantly, has resulted in applications of shear connectors in a variety of structures utilizing a number of different steels. Basic research work on composite construction was carried out several years ago, but the increased interest in this structural system has caused renewed interest in a number of questions not answered in the earlier studies.

Most of the research work conducted in the past has been carried out primarily for one of two purposes. Push-out tests (1) designed to determine the shear capacity of the many varieties of connectors and to study the load transfer distribution constitute the most common investigations. The second most common type of study has been conducted to determine the static flexural strength of composite beams. Very few fatigue tests were included in the earlier work.

This situation is not surprising since in most applications of composite construction the shear connectors are attached to a steel flange subjected to flexural stresses which are usually compressive or, at most, very small tensile stresses. In this case the fatigue problem is associated with the connector itself. The interest in the use of composite construction along the entire length of continuous structures and the desire to use higher strength steel in many applications has raised questions in connection with the fatigue resistance of such structures.

In these latter applications, a sufficient margin of safety must be provided to preclude fatigue failure of the flange of the beam. Shear connectors attached to the tension flange or to high-strength steels where a larger stress range is possible could serve as points of initiation for progressive failure. The program reported herein was undertaken to study this problem.

The primary objective of this program was to study the effect of shear connectors on the fatigue life under circumstances where the connectors are attached to the tension flange and to study the influence of flange material on this behavior. To study these two problems, work was undertaken on several different materials with varying chemical compositions and with different strength levels.

The program included a rather extensive series of tests on flat plate-type specimens. These specimens were fabricated from two different materials. For the different types of materials studied, one or more stud shear connectors were attached in a single line transverse to the direction of stress. Another variable, intended to permit a study of the effect of stud spacing, was the width of the plate. In one series of tests the welding procedure used to apply the studs was altered.

Flat-plate fatigue tests were conducted on stress cycles of complete reversal, zero-to-tension and partial tension-to-tension. A few supplementary tests were conducted to investigate the effect of geometry in the region of the connection between the plate and the stud shear connector.

The second phase of the program was carried out on nine beam specimens, divided into three groups of three beams each. All beams were loaded so that the flange to which the stud shear connectors were attached was subjected to a tensile stress. The first group of beams was tested without any stress applied to the shear connectors.

Paper sponsored by Committee on Bridges.

This series could then be directly related to the flat-plate tests to study the effect of stress gradient.

Bending of the beam and flexing of the stud simultaneously were studied in the other two series of beam tests. Two different methods were used to accomplish this loading condition. The studs of one group of beams were loaded by pre-tensioned mechanical flexors fabricated specifically for this purpose and provided with strain gages to monitor the load. In the final group of beams, a reinforced concrete slab was cast to resemble the situation as it actually exists in practice.

DESCRIPTION OF MATERIALS AND TESTS

Materials

Three different steels were used in the fabrication of the flat-plate and beam specimens reported herein. These three steels are referred to in the following discussion by their ASTM designations.

A7F Steel. —During the initial phases of the study reported, one series of eight plate specimens (GIA series) was fabricated from a steel which was available in the laboratory and had been purchased some time earlier to conform to ASTM A7-58T. Coupon tests carried out in the laboratory indicated that this steel failed to meet the tensile requirements of this specification.

A441 Steel. —All remaining flat-plate tests were carried out on specimens fabricated from a steel which satisfied the requirements of ASTM A441-60T. This material was also used as the flange material in the beam tests.

A373 Steel. —The third type of steel used served for the web material of the nine beam specimens. This steel met the requirements of ASTM A373-58T. Due to the location of this material in the beam specimens and the type of tests being conducted, this steel did not affect the fatigue life being studied.

The chemical composition and physical properties of all base materials are presented in Table 1. All specimens were fabricated in the Civil Engineering Shop at the University of Illinois and then shipped to Gregory Industries, Inc., in Lorain, Ohio, where the studs were affixed.

The entire test program was broken down into five different series of tests, designated GIA through GIE. Each specimen received a designation consisting of three letters to indicate the specific series followed by a number to distinguish the particular test specimen within that series (e.g., GIB12).

Plate Specimens

The dimensions of the various plate specimens are shown in Figures 1, 2 and 3. The details of the welding procedure used in the application of the studs to the individual specimens are given in Table 2.

GIA Series. —This series consisted of eight plate specimens machined from A7F steel. Each specimen was machined to the dimensions shown in Figure 1a before the stud was attached. Each specimen was provided with a single stud on a $3\frac{1}{2}$- by $\frac{1}{2}$-in.

TABLE 1

PROPERTIES OF BASE MATERIALS

Steel	Chemical Composition								Yield Pt.[a] (ksi)	Tensile[a] Strength (ksi)	Elongation[a, b] (%)
	C	Mn	P	S	Si	Cu	Va	Ni			
A7F[c]	0.20	0.28	0.009	0.041	0.01	0.05	-	0.01	30.3	52.8	29.5
A373	0.23	0.63	0.022	0.031	0.030	0.17	-	-	38.8	64.8	29.6
A441	0.20	1.14	0.015	0.031	0.06	0.23	0.06	-	61.6	84.1	22.2

[a]Based on average of three tests.
[b]Per 8 in.
[c]Failed to meet ASTM A7 tensile requirements.

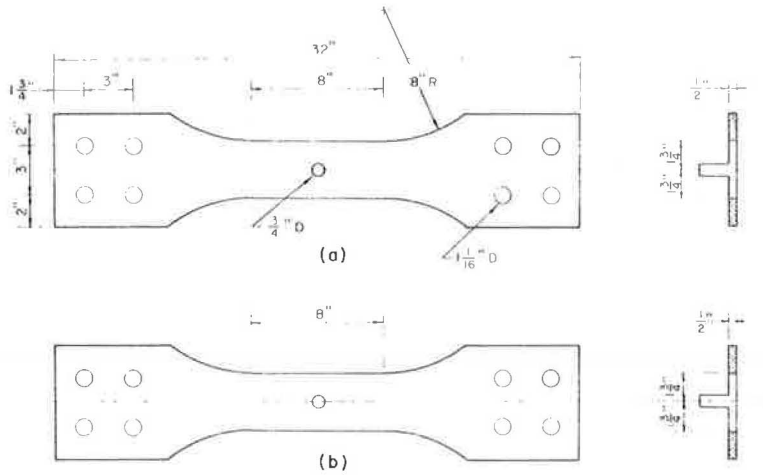

Figure 1. Dimensions of small plate specimens: (a) GIA specimens, and (b) GIB specimens.

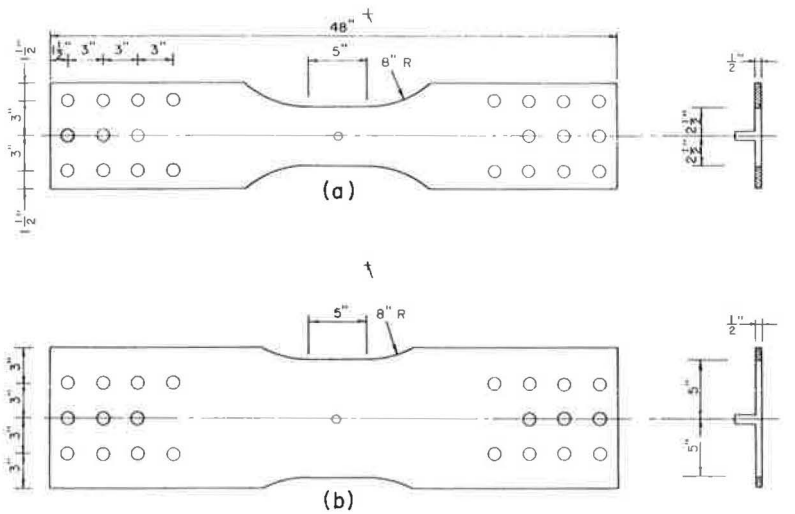

Figure 2. Dimensions of large plate specimens with a single stud: (a) GIC specimens, and (b) specimens GID1 through GID3.

cross-section. Throughout all five series, the material thickness was maintained constant at ½ in. to reduce the number of variables involved.

GIB Series.—Basically, the GIB series, involving 20 specimens, was identical in all respects to the GIA series except that A441 steel was used instead of A7F. Specimens GIB16 through GIB20 were subjected to a slightly different welding procedure and several specimens had slight variations in geometry.

GIC Series.—The only significant difference between the five GIC specimens and those of the GIB series was the width of the cross-section. In this series of tests the width was increased to 5 in. Both series were fabricated from A441 steel and contained a single stud attached at the center of the flat-plate specimen.

GID Series.—To study the effect of multiple studs, ten flat-plate specimens were machined to a 10 in. width across the test section. These specimens were then provided with either one, three, or five studs attached in a single line transverse to the

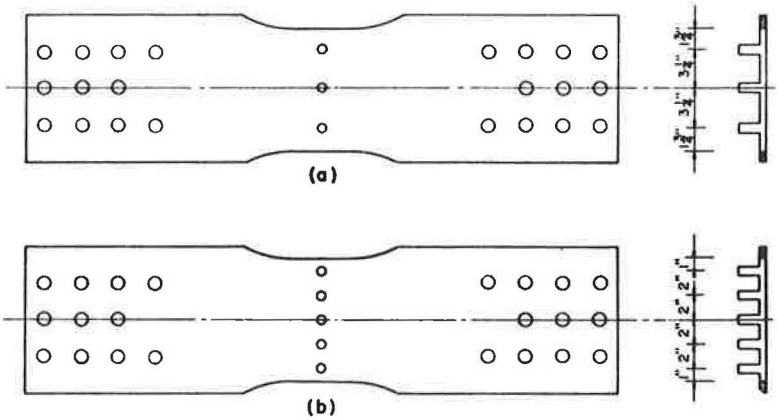

Figure 3. Dimensions of large plate specimens with multiple studs: (a) specimens GID4 through GID6, and (b) specimens GID3 through GID10.

TABLE 2

STUD-WELDING PROCEDURES

Specimens	Lift (in.)	Plunge (in.)	Weld Current (amp)	Arc Voltage (volts)	Weld Time (cycles)
GIA1-GIA8	3/32	3/16	1500	33	58
GIB1-GIB15	3/32	3/16	1500	33	58
GIB16-GIB20	3/32	3/16	1450	33	76
GIC1-GIC5	3/32	3/16	1750	31	43
GID1-GID10	3/32	3/16	1750	31	43

direction of applied stress. In addition to the increased width, these specimens, as well as those of the GIC series, were 4 ft long, whereas specimens of the GIA and GIB series were only 2 ft 8 in. long. The difference in length was necessitated by the increased cross-sectional area which required loadings of such a magnitude that they could only be produced by the larger testing machines.

The cross-sections of all flat-plate specimens through the line of studs are shown in Figure 4.

Beam Specimens

The nine steel beams used in this phase of the investigation were fabricated from three flat plates. The beams had an overall depth of 12 in., a flange thickness of $\frac{1}{2}$ in., and a web thickness of $\frac{3}{16}$ in. Each of the beams was then provided with two rows of studs spaced $2\frac{1}{2}$ in. apart. Each of the rows contained nine studs at a spacing of 10 in. along the length of the beam. These nine specimens were then subdivided into three groups of three specimens each and subjected to different loading conditions.

Specimens GIE1 through GIE3 were tested as simple flexural members with no external loads applied to the stud shear connectors. Specimens GIE4 through GIE6 were altered in such a manner as to remove the heads from the eight centrally located studs. Specially prepared and calibrated connectors were placed over four pairs of studs as shown in Figure 5b. These connectors were made so that they could be pretensioned to produce any desired shear force in the studs. The force in the connector was measured by strain gages attached to the connector and calibrated in a static testing machine. Additional strain gages were attached to specimens GIE4 and GIE5 to determine the strain distribution across two different cross-sections. The output from

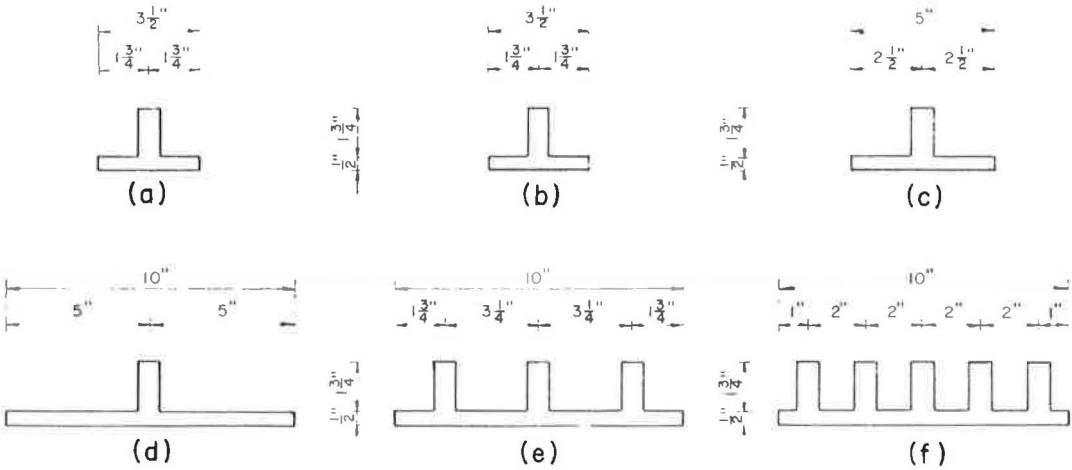

Figure 4. Cross-sections of flat-plate specimens through line of studs: (a) GIA, (b) GIB, (c) GIC, (d) GID1 through GID3, (e) GID4 through GID6, and (f) GID7 through GID10.

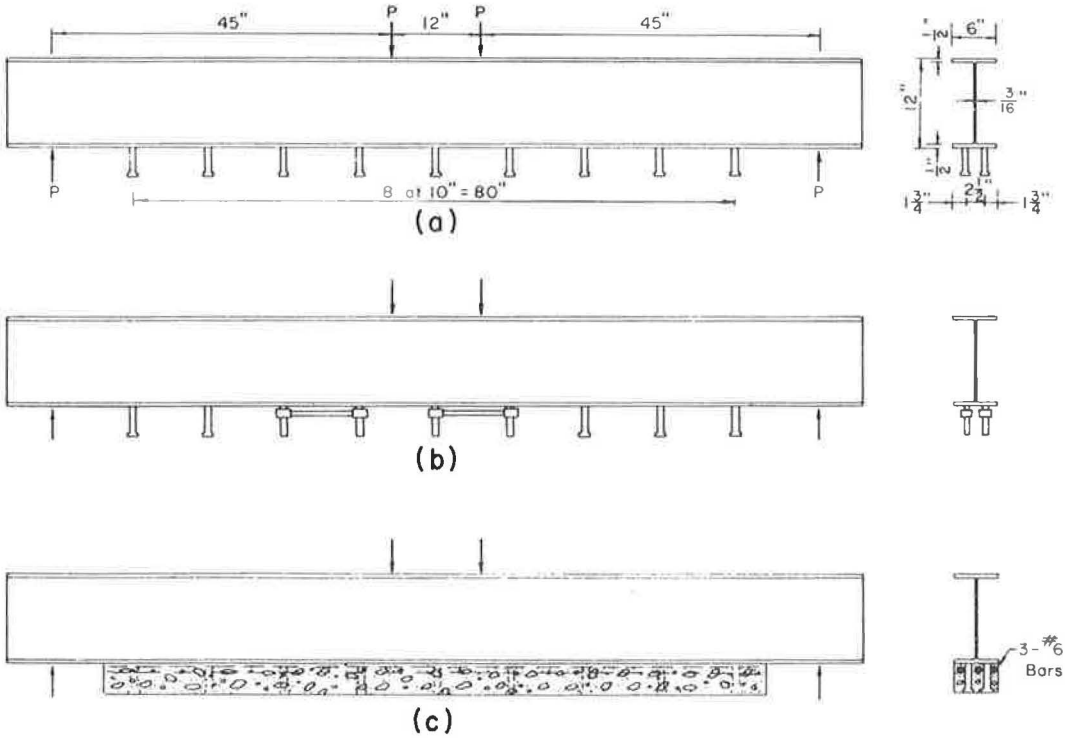

Figure 5. Details of beam specimens: (a) GIE1 through GIE3, (b) GIE4 through GIE6, and (c) GIE7 through GIE10.

these strain gages was recorded during the period of the fatigue test on a Sanborn recorder.

The studs of specimens GIE7 through GIE9 were incased in a reinforced concrete slab as shown in Figure 5c. A mixture of graphite and linseed oil (one part graphite to 4.4 parts of linseed oil) was placed on the steel surface to destroy the steel-concrete bond. In this way all of the shear force must be transmitted through the studs. The reinforcing steel consisted of three No. 6 bars located ¾ in. below the lower flange of the steel beam. Beams GIE7 and GIE9 were instrumented with strain gages at various locations and through the depth of the steel beam to determine the strain distribution through the depth and the extent to which this strain distribution was altered as a result of the shear force transmitted through the shear connector.

Object of Individual Test Series

GIA Series. —The purpose of this series of tests was to obtain a basic S-N curve for A7F steel on a zero-to-tension stress cycle so that these results could be compared with similar tests on A441 steel.

GIB Series. —In this series S-N curves were to be established for both zero-to-tension stress cycles and a fully reversed stress cycle. On the basis of the results obtained on these two series of tests, an estimate was made of the stress cycle which would produce failure at 2,000,000 cycles on a one-half tension-to-tension stress cycle.

Specimens GIB16 through GIB20 were produced with a slightly different stud welding procedure from the rest of the specimens in this series. The purpose of these specimens was to investigate the effect of altering the stud welding procedure on the fatigue life and the fatigue behavior of this material. Two specimens, GIB11 and GIB12, were subjected to additional treatment after the studs had been attached. This treatment consisted of grinding the upset to produce a smooth transition from the plate to the stud to evaluate the significance of the geometry of the upset.

In two other specimens, GIB19 and GIB20, the studs were completely removed by grinding. The grinding was carried out so as to approximate the surface condition of the surrounding plate as nearly as possible. In these cases the notch effect of the upset and the presence of the stud had been completely removed, so that any difference in the results from plain-plate test results would indicate the effect of welding on the base material.

The tensile strength of GIA and GIB series specimens was checked by three static tests providing a basis for comparison of the various fatigue strengths with the static ultimate strength of similar specimens.

GIC Series. —The function of this series was to determine the fatigue strength for failure at 2,000,000 cycles on a one-half tension-to-tension stress cycle. Specimens in this series were 5 in. wide so that a comparison with the results of the GIB series would give some indication of the size effect. Specimen GIC5 was not subjected to any fatigue loading but was examined metallurgically to determine the hardness distribution near the stud.

GID Series. —All of these specimens were tested under a one-half tension-to-tension stress cycle. Specimens were provided with either one, three, or five studs on a single line transverse to the direction of applied stress. In all cases the fatigue strength for failure at 2,000,000 cycles was desired. The single-stud specimens, GID1 through GID3, provided data for a further evaluation of the effect of width since the cross-section was 10 in. wide in this series. Comparison of the three groups of specimens within this series provides an evaluation of stud spacing.

GIE Series. —This series was divided into three groups of three beams each. In every case the fatigue strength for 2,000,000 cycles under a one-half tension-to-tension stress cycle was desired. The purpose of the first group of tests, GIE1 through GIE3, was to compare the fatigue strength of the flange with the attached studs with the results of the axially loaded plate specimens. The other two groups were intended to show the effect of transmission of shear force through the stud connector while the beam is being subjected to primary bending. This, of course, is the loading condition occurring in actual composite construction. Some strain gages were attached to

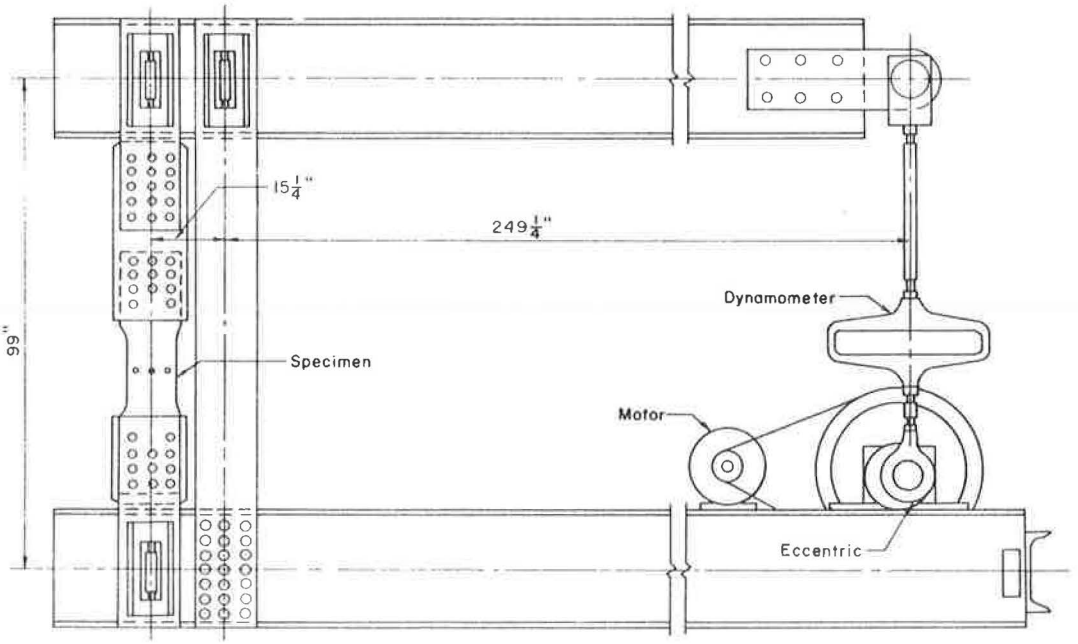

Figure 6. Illinois' fatigue testing machine for axial loading.

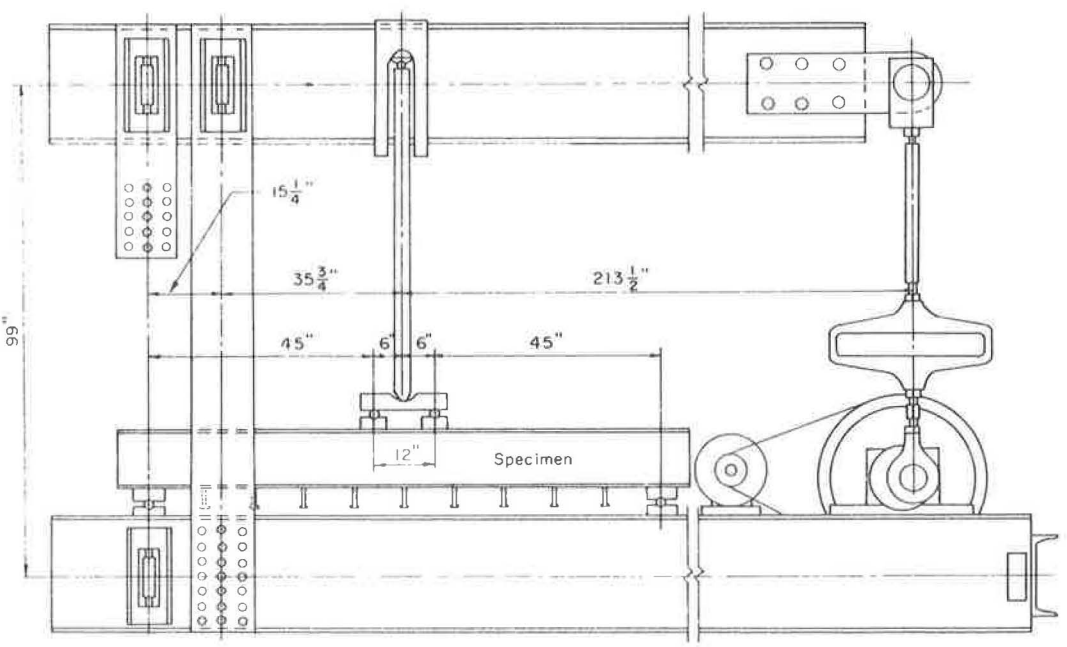

Figure 7. Illinois' fatigue testing machine modified for flexural loading.

several of these specimens to check the strain distribution across several cross-sections.

Test Procedures

All fatigue tests were conducted in University of Illinois lever-type fatigue machines. The small plate specimens, GIA and GIB series, were tested in machines with a total load capacity of 50,000 lb and all other tests were conducted in the larger 200,000-lb machines. These machines, while similar in their basic operation, varied in speed from 300 to 100 cycles/min.

Schematic diagrams of the University of Illinois fatigue testing machine adapted for axial or flexural loading can be seen in Figures 6 and 7, respectively. By adjusting the variable throw eccentric and the turnbuckle immediately above it, the required stress cycle can be applied to the specimen. The load is determined by an Ames dial which measures the deformation of the dynamometer.

A microswitch near the specimen end of the machine is adjusted so that excessive deflection of the specimen trips the switch and stops the machine. During the progress of the fatigue fracture the load is adjusted so that the specimen is subjected to a relatively constant load. Failure is defined as having occurred when the specimen could no longer withstand the prescribed load without yielding.

Before testing, the plate specimens were measured to determine the average cross-sectional area at the position of the stud. This area was then used to determine the load so that the desired average stress would exist at the expected failure location. In the case of the beam specimens, the loads and, therefore, the moments acting on the beam were calculated by the deformation of the dynamometer. The stresses were obtained by the simple flexural formula using the moment of inertia computed for the fracture section.

TABLE 3

FATIGUE RESULTS, ZERO-TO-TENSION, AXIAL LOADING

Specimen	Stress Cycle (ksi)	Life (cycle)
GIA1	0 to +16.5	1,320,000
GIA2	0 to +24.0	460,000
GIA3	0 to +24.0	840,000
GIA4	0 to +20.0	1,170,000
GIA5	0 to +16.5	1,480,000
GIA6	0 to +16.5	2,250,000
GIA7	0 to +15.0	3,240,000[a]
GIB1	0 to +20.0	820,000
GIB2	0 to +16.5	1,460,000
GIB3	0 to +16.5	2,410,000
GIB4	0 to +15.5	2,510,000
GIB11[b]	0 to +16.5	4,200,000
GIB12[b]	0 to +20.0	2,060,000
GIB16[c]	0 to +16.5	1,920,000
GIB17[c]	0 to +16.5	1,610,000
GIB19[d]	0 to +28.0	4,940,000[a]
GIB19[d]	0 to +40.0	810,000
GIB20[d]	0 to +38.0	550,000

[a]Did not fail.
[b]Upsets ground to form smooth transition.
[c]Welding procedure altered.
[d]Welding procedure altered and studs removed.

BEHAVIOR OF FLAT-PLATE SPECIMENS

The results of individual tests carried out on the plate specimens are given in Tables 3 through 6. These same results are shown as S-N diagrams in Figures 8 through 12. The data indicate a minimum amount of scatter and good consistency among the results.

The fatigue results showed amazingly little scatter so that relatively few tests gave a strong indication of the fatigue resistance of plate specimens with attached studs. Most of the tests carried out were intended to determine the magnitude of the stress cycle which would result in failure at 2,000,000 cycles. A study of the various S-N diagrams indicates that such stress cycles are as follows: for complete reversal a stress cycle from 8.0-ksi compression to 8.0-ksi tension (a range of 16.0 ksi), for the zero-to-tension stress cycle from 0 to 16.0 ksi (a range of 16.0 ksi), and for a stress cycle ranging from one-half tension-to-tension from +14.0 to +28.0 ksi (a range of 14.0 ksi). It should be

noted that the stress range remains almost constant as the stress cycle changes.

Influence of Base Material on Fatigue Life

An indication of the effect of variations in base material is obtained by comparing the results of the GIA and GIB specimens. Figures 8 and 9 present the results for specimens which are similar in all respects except for base material. Seven GIA specimens, fabricated from A7F steel, and six GIB specimens, fabricated from A441 steel, were subjected to a zero-to-tension stress cycle. For each group of tests the results formed a very narrow scatter band, as indicated on the figures. When the data are superimposed, the two scatter bands coincide almost perfectly, as is seen in Figure 10. It must be noted that this excellent correlation involved only a few tests of two steels for one particular type of stress cycle. These results are similar to results previously obtained on these materials in studies of the effect of butt-welded joints.

Effect of Stud-Welding Procedure

To study the effect of variations in the stud-welding procedure, five specimens of the GIB series were fabricated with a substantially different welding procedure from that used for the preparation of the remainder of these specimens. For specimens GIB16 through GIB20, the weld current was 1,450 amperes, the arc voltage was 33 volts, and the weld time was 76 cycles. The remainder of the series, specimens GIB1 through GIB15, were prepared with a weld current of 1,500 amperes and an arc voltage of 33 volts for 58 cycles. This means simply that specimens GIB15 through GIB20 were subjected to 26 percent more heat than other specimens of this type.

Two of these specimens, GIB16 and GIB17, were subjected to a zero-to-tension stress cycle in the as-produced condition. The results of these tests are presented in Figure 9 and no significant difference in fatigue life was obtained. One specimen, GIB18, was subjected to a one-half tension-to-tension stress cycle in the as-welded condition and a study of the results given in Table 5 indicates that

TABLE 4

FATIGUE RESULTS, COMPLETE REVERSAL, AXIAL LOADING

Specimen	Stress Cycle (ksi)	Life (cycles)
GIB5	-20.0 to +20.0	190,000
GIB6	-20.0 to +20.0	180,000
GIB7	-10.0 to +10.0	960,000
GIB8	- 8.5 to + 8.5	1,730,000
GIB9	- 8.5 to + 8.5	1,660,000

TABLE 5

FATIGUE RESULTS, ONE-HALF TENSION-TO-TENSION, AXIAL LOADING

Specimen	Stress Cycle (ksi)	Life (cycles)
GIB13	+14.0 to +28.0	1,950,000
GIB14	+14.0 to +28.0	2,560,000
GIB15	+14.0 to +28.0	2,140,000
GIB18[a]	+14.0 to +28.0	2,690,000
GIC1	+27.9 to +55.8	280,000
GIC2	+14.0 to +28.0	2,220,000
GIC3	+14.0 to +28.0	2,700,000
GIC4	+14.0 to +28.0	2,590,000

[a]Welding procedure altered.

TABLE 6

FATIGUE RESULTS, ONE-HALF TENSION-TO-TENSION, AXIAL LOADING

Specimen	No. of Studs	Stress Cycle (ksi)	Life (cycles)
GID1	1	+14.0 to +28.0	3,260,000[a]
GID1	1	+15.0 to +30.0	1,730,000
GID2	1	+14.0 to +28.0	2,710,000
GID3	1	+15.0 to +30.0	1,840,000
GID4	3	+14.0 to +28.0	1,630,000
GID5	3	+14.0 to +28.0	1,900,000
GID6	3	+14.0 to +28.0	1,890,000
GID7	5	+14.0 to +28.0	1,410,000
GID8	5	+14.0 to +28.0	1,880,000
GID9	5	+14.0 to +28.0	1,570,000
GID10	5	+14.0 to +28.0	1,460,000

[a]Specimen did not fail.

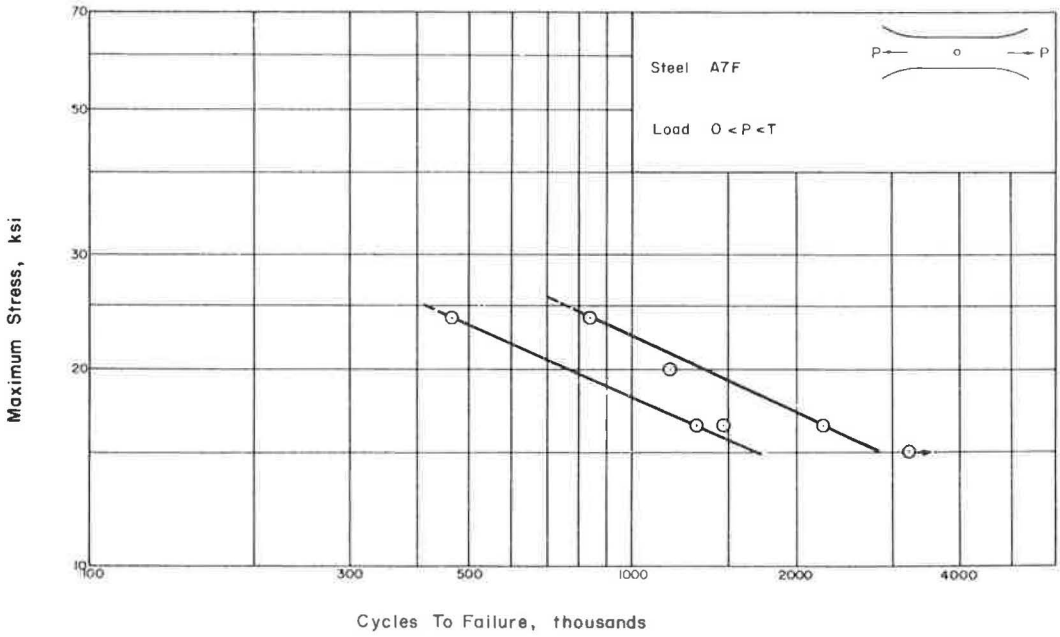

Figure 8. Fatigue results for GIA specimens, zero-to-tension stress cycle.

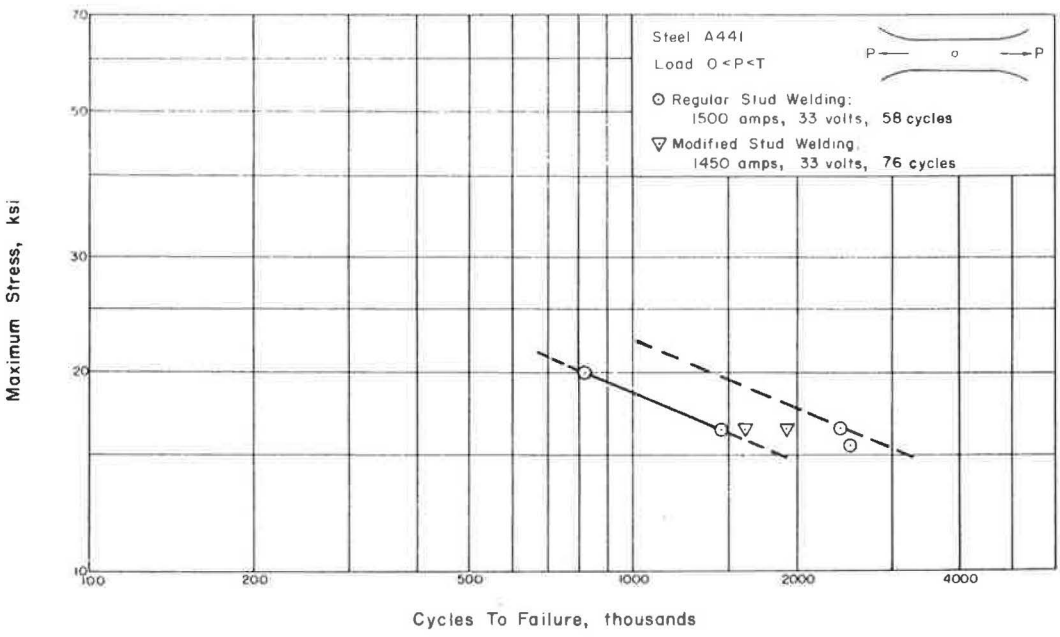

Figure 9. Fatigue results for GIB specimens, zero-to-tension stress cycle.

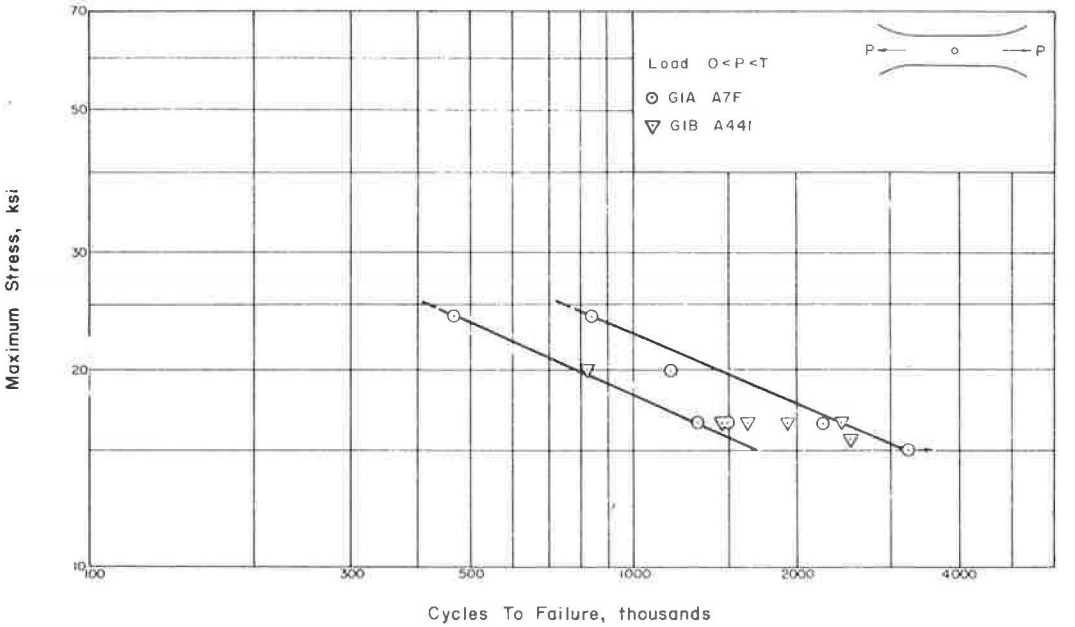

Figure 10. Effect of type of steel on fatigue life, zero-to-tension stress cycle.

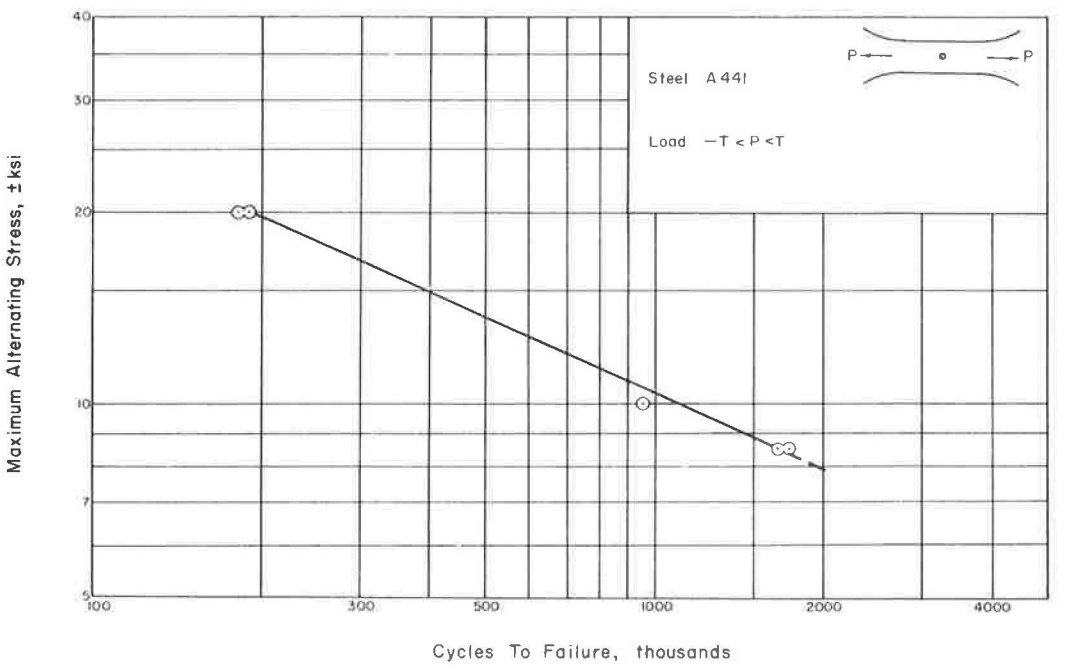

Figure 11. Fatigue results for GIB specimens, complete reversal stress cycle.

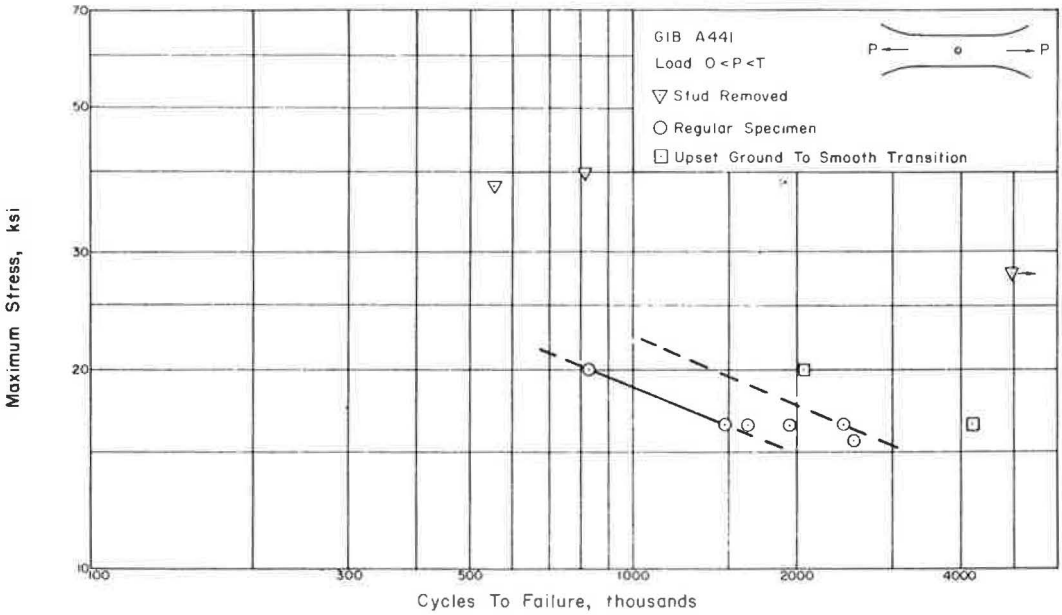

Figure 12. Geometrical effect on fatigue results, zero-to-tension stress cycle.

no significant difference could be observed. The remaining two specimens with the modified welding procedure, GIB19 and GIB20, were subjected to special tests which are reported later.

On the basis of the tests conducted it can be concluded that, within the limits studied, the variations in welding procedure had no significant effect on the fatigue life.

Effect of Upset Geometry

To study the effect of geometry in the region of the upset, four specimens of the GIB series were subjected to treatments altering this geometry. Two specimens, GIB11 and GIB12, were ground so that their upsets formed a smooth transition from the plate surface to the stud. Each was tested at a different zero-to-tension stress cycle for which results were available for specimens with the as-produced geometry. The results of these tests are presented in Table 3 and Figure 12. Figure 12 indicates that the fatigue life of these treated specimens was approximately double that of the as-produced specimens.

The studs of two other specimens of this series, GIB19 and GIB20, were completely removed and the surface smoothness was ground to approximate that of the surrounding plate. This alteration should remove completely the geometrical effect and, therefore, any difference in fatigue life between these specimens and plain plate specimens could be attributed to the effect of welding on the base metal. The results of the tests conducted on these two specimens are given in Table 3. The specimens proved to be significantly more fatigue resistant than all other types of specimens in this program. These test results are not quite as good as the results obtained in previous investigations for plain plate specimens of A441 steel. Therefore, one can conclude that even when the stud is completely removed from the plate to which it is attached, some effect of the welding remains and the fatigue resistance is slightly less than that obtained for plain plate material.

Significance of Stud Spacing

The effect of stud spacing can be studied by comparing several different series of tests. In one case, the effect of plate width can be studied for the various specimens

provided with a single stud. Series GIB, GIC, and GID all contain test results for single-stud specimens subjected to a one-half tension-to-tension stress cycle. The results of these tests are given in the individual tables and have been presented for purposes of comparison in Figure 13. These results indicate that a slight increase in fatigue life is obtained when the width of the plate is increased. Although the plate to which the stud is attached is continuous, the stud acts somewhat like a hole in a flat-plate specimen. The stress concentration effect increases as the width of the plate decreases, which is directly in line with what would be expected for a plate with a hole.

The effect of stud spacing can also be studied by examining the results of the GID series (Table 6, Fig. 14). All tests in this series were conducted on a stress cycle which varied from one-half tension-to-tension. The specimens were all 10 in. wide and were provided with one, three, or five studs. In the multi-studded specimens, it might easily be reasoned that since the plate is heated and cooled more slowly when several studs are attached in succession, the plate should contain residual stresses of a lower magnitude and the studs should represent less of a stress concentration. However, one could easily argue in favor of a reduced fatigue life because of the increased number of stress concentrations where fatigue fracture could initiate.

An examination of the test results indicate that neither of these factors is very dominant. As seen in Figure 14, the single-studded specimens are slightly more resistant to fatigue failure. However, a study of the results presented in Figure 13 reveal that the results for a single stud attached to a $3\frac{1}{2}$-in. wide plate, corresponding to a stud spacing of $3\frac{1}{2}$ in., and the results for the single stud attached to a 5-in. wide plate, corresponding to a stud spacing of 5 in., give results in line with those presented in Figure 14. Although there is a slight decrease in fatigue life as the number of studs in any one line is increased, this difference is not significant when converted to stress levels which would produce failure at the same number of cycles.

It is interesting to note at this time that the specimens with more than one stud attached always had more than one failure surface occurring independently and almost

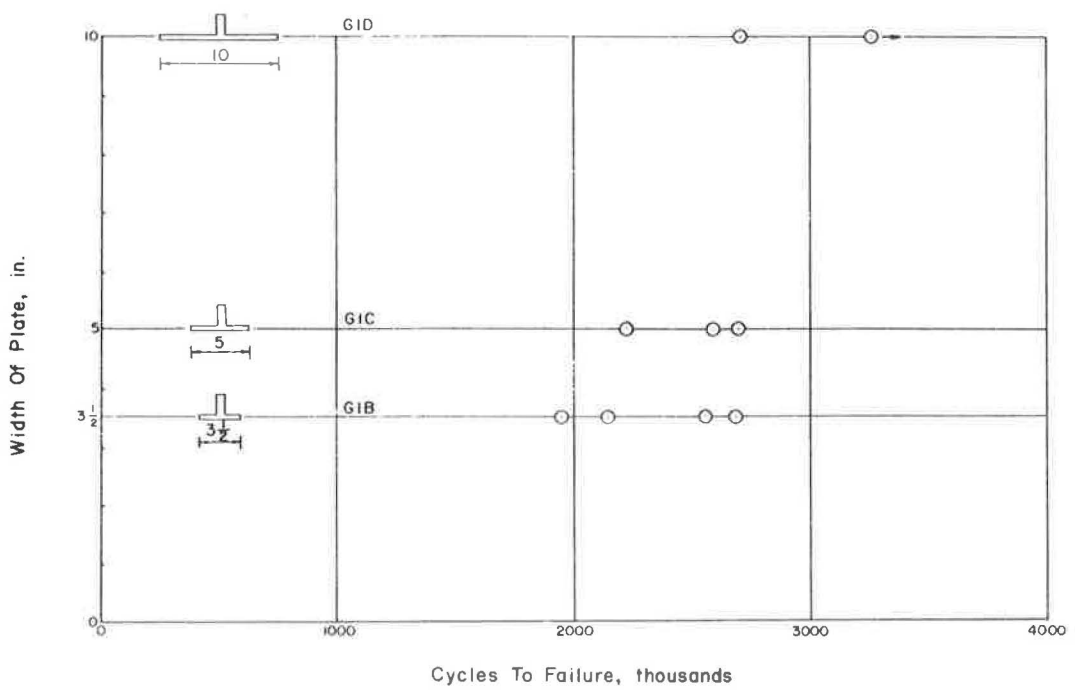

Figure 13. Width of plate vs fatigue life, stress cycle +14.0 to +28.0 ksi.

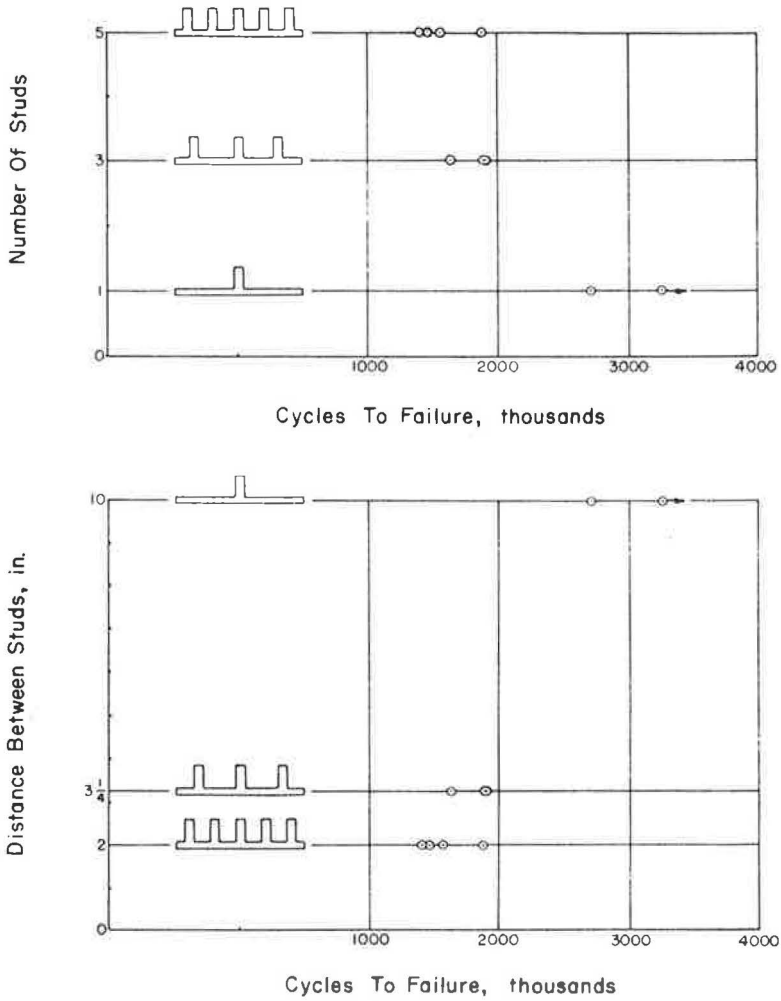

Figure 14. Stud spacing vs fatigue life, stress cycle +14.0 to +28.0 ksi.

simultaneously. In a number of cases, failures occurred above and below the same stud. These fractures indicate that failure is not precipitated by one particular weak spot, but that the effect of the studs is extremely consistent and that failures initiate at a number of independent locations and propagate individually.

Comparison with Other Test Results

Table 7 gives test results obtained in this and previous investigations (2, 3) with similar materials. Previous tests have been conducted on plain-plate material of A441 and A7, double-V butt-welded joints in A441 steel and plate material with a single hole. These results indicate that the attachment of studs is a somewhat more severe condition than the presence of a hole or of a double-V butt weld. On the basis of the results for plain-plate specimens of A441, the plate with studs has an effective stress concentration factor in fatigue of approximately 2.5.

Static Tests

During the course of the investigation several static tests on plain-plate specimens with a single attached stud were conducted. The results of these tests (Table 8)

TABLE 7

EFFECT OF VARIOUS STRESS RAISERS ON FATIGUE LIFE OF PLATE SPECIMENS[a]

Specimen	$F_{2,000,000}$ (ksi)
Plain plate (A441)	0 to +40
Plain plate (A7)	0 to +35
Double-butt weld (A441)	0 to +28
Plate with hole (A441)	0 to +24
Plate with stud (A441)	0 to +16

[a]Zero-to-tension, axial loading.

TABLE 8

RESULTS OF STATIC TESTS

Specimen	ASTM Designation	Yield Point (ksi)	Ultimate Strength (ksi)
GIA7	A7F[a]	31.6	53.9
GIA8	A7F[a]	29.6	53.6
GIB10	A441	-	80.4

[a]Failed to meet ASTM A7 tensile requirements.

indicate that the presence of the stud did not in any way influence either the yield point or the ultimate strength of the base material. A comparison of these results with those presented in Table 1 indicates that the average of the yield point obtained is at least as high as that obtained on the coupon tests and the ultimate strength is somewhat higher. With the A441 specimen no yield point was recorded, but the ultimate strength is very close to that obtained in the coupon tests and is well in excess of that required by the specifications.

BEHAVIOR OF BEAM SPECIMENS

The purpose of this series of tests was to provide a correlation between the results of the flat-plate specimens and the stress conditions as they actually occur in composite construction. In addition, as previously noted, this series of specimens was divided into three groups: one subjected to flexural loading without any load being transmitted through the stud shear connector, one subjected to flexural loading with a shear loading applied by special mechanical adapters and a final group in which the stud was embedded in a concrete slab and subjected to shear force transmitted by the composite action obtained. All tests on beam specimens were conducted on a stress cycle which ranged from approximately one-half tension-to-tension with the stress range chosen so as to produce failure in approximately 2,000,000 cycles. The results are presented in Table 9.

Plain-Beam Tests

The results of the plain-beam tests, specimens GIE1 through GIE3, indicate that a stress cycle alternating between 16.4- and 32.8-ksi tension is required to produce failure in approximately 2,000,000 cycles. This stress range is slightly higher than the stress range which produced failure at this same life in the plain-plate specimens. Although no direct comparison can be made since the flange used in the beam tests was provided with two studs on a 6-in. wide plate and a spacing between studs of $2\frac{1}{2}$ in., the results can be compared with specimens of the GIC series and the GID series. In the GIC series a single stud was attached to a 5-in. wide plate, in the GID series specimens providing stud spacings of $3\frac{1}{4}$ and 2 in. are included.

In all of the cases referred to, a stress cycle ranging from 14.0 to 28.0 ksi produced failure in approximately 2,000,000 cycles. This slight increase in stress cycle to produce failure in 2,000,000

TABLE 9

FATIGUE RESULTS FOR BEAM SPECIMENS ONE-HALF TENSION-TO-TENSION, FLEXURAL LOADING

Specimen	Type[a]	Stress Cycle (ksi)	Life (cycles)
GIE1	PB	+15.0 to +29.9	2,780,000
GIE2	PB	+16.4 to +32.8	2,070,000
GIE3	PB	+16.5 to +32.9	1,940,000
GIE4	SF	+11.5 to +24.2	2,020,000
GIE5	SF	+12.4 to +24.6	2,210,000
GIE6	SF	+12.7 to +25.2	1,830,000
GIE7	RC	+10.7 to +21.4[a]	1,480,000
		+15.0 to +30.0[a]	610,000
GIE8	RC	+15.0 to +30.0[a]	1,640,000
GIE9	RC	+15.3 to +30.0[a]	1,500,000

[a]PB - plain beam, SF - stud flexors, and RC - reinforced concrete.
[b]Based on Mc/I where I assumes concrete is cracked.

cycles in the beam specimens is in all probability attributable to the stress gradient existing through the flange and the relief provided for the stress concentration effect of the stud. Even if one compares the average stress across the total flange area, the stress range for the beams in the current series of tests was from 15.7 to 31.4 ksi.

These results are extremely encouraging because they indicate that tests carried out on plain-plate specimens give an excellent indication of the strength which can be expected of similar installations on beams.

Beams with Stud Flexors

Specimens in this series were identical in all respects to those in the previous group, except that a shear force was applied to several of the stud shear connectors by a mechanical attachment. As mentioned earlier the heads of several studs near the center of the beam were removed so that mechanical flexors could be attached. Load in the flexors was adjusted by strain gages. A photograph of the flexor used for this purpose and a view of one beam with flexors in place are shown in Figure 15. The load applied was located approximately ¾ in. from the surface of the flange.

At the beginning of the fatigue test, the load in the flexor was adjusted so that at a maximum flexural load the shear stress in the studs to which the flexor was attached had a nominal value of 15,000 psi. All beams were tested on a stress cycle which varied from one-half tension-to-tension. The load in the flexor, however, remained nearly constant at the magnitude applied at the beginning of the test. The load in the flexor could be monitored during the individual test cycles and also at various stages during the progress of the test. Such monitoring indicated that at no time during the course of a test on any specimen did the load in the flexor drop below a value of 80 percent of the maximum value set. In only a few cases did the load on the flexor drop to this value. In the other cases, the load in the flexor did not drop below a value of 85 percent of the maximum value. This fact is particularly significant because the stress levels reported in Table 9 are computed on the basis of the section properties of the base beam at the location of the failure. No account has been taken of the effect of the stud flexor on the distribution of stress through the depth of the beam. The local effect of the load transmitted through the stud has also been neglected in the stresses reported.

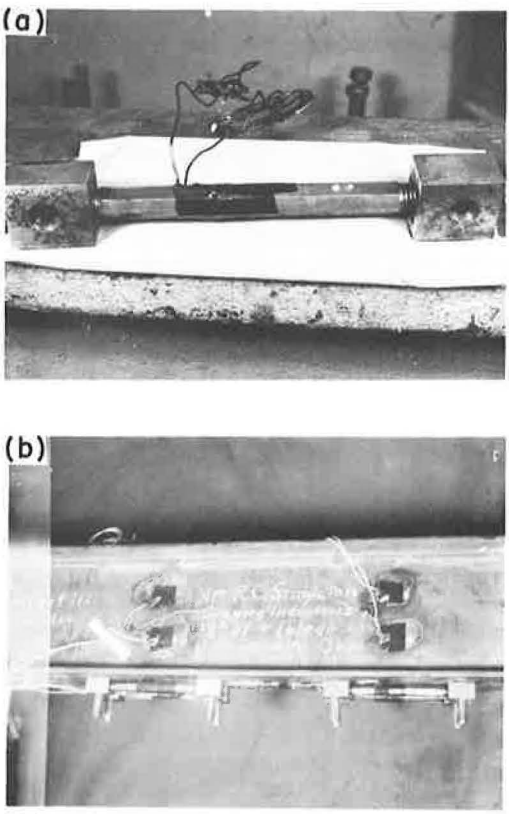

Figure 15. Mechanical stud flexors: (a) flexor, and (b) beam with stud flexors in position.

All failures in this series of beam specimens occurred on the side of the stud away from the flexor used to apply load to the stud. Two failures occurred at the centerline of the beam where the moment and corresponding flexural stress have the maximum value. The other failure occurred at a stud at a distance of 10 in. from the centerline of the beam. At this point, the moment and flexural stress have a value equal to 91 percent of the maximum value at midspan. Since these values are based on nominal stress calculations and neglect the local effect of

the load in the stud, the actual difference in stresses for these two fracture locations must be even smaller than that indicated by simple flexural calculations.

The foregoing discussion serves to explain why the stresses reported in Table 9 for this particular series appear to be somewhat low. With the load transmitted through the stud, however, these beams still required a stress range of about 12.5 ksi on a one-half tension-to-tension stress cycle to produce failure in 2,000,000 cycles.

Beams with Reinforced Concrete Cover

All beams in this series were provided with a reinforced concrete cover. The amount of reinforcement placed in the concrete was calculated to produce in the studs a maximum shear force equal in magnitude to the maximum load applied in the previous series by the mechanical flexors. The reinforcement was placed in one layer near the tension flange, resulting in the proper magnitude of shear force in the studs and a distribution of flexural stresses in the base beam to insure failure under the applied loads in approximately 2,000,000 cycles.

Specimens in this series, as in the previous series, were provided with strain gages at several locations along the length of the beam. The strain gages were distributed through the depth of the beam to indicate the extent to which the concrete and the reinforcement acted as a composite section. These gages were located at cross-sections corresponding to the location of studs and at the section midway between the studs.

On application of load during the progress of the fatigue test, cracks appeared at each row of studs. These were the only visible concrete cracks which formed during the course of the fatigue tests; their presence caused fluctuations in the location of the neutral axis as determined from the strain gages.

In the region between studs where the concrete was not cracked, the neutral axis was shifted toward the flange to which the shear connectors were attached. At the stud locations where the concrete was cracked, the neutral axis shifted slightly away from the tension flange of the beam. Near the ends of the span, between the rows of studs, the neutral axis shifted to a location which indicated that the concrete in this region is almost completely effective.

For beams in this series the nominal stress on the extreme fiber of the tension flange can be computed in several different ways, depending on the basis used for these calculations. One can assume that only the steel beam resists the bending moment, in which case the stress cycle for beams GIE7, GIE8 and GIE9 in the fatigue test was from +21,800 to +43,800 psi for a total range of 22,000 psi.

The stress cycles reported in Table 9 were calculated on the basis of a cracked section for all of the concrete slab. On the basis of the results of the strain gage studies, this is the most reasonable assumption for the actual state of stress. A very reasonable check on these stresses was obtained by the strain gages. These gages indicated a linear strain distribution throughout the web of the beam. In both flanges the strain recorded by the gages was less than the value which would be expected if the web strains are extrapolated. This nonlinearity is caused by local effects on both flanges. In one flange the indicated strains are affected by the presence of the loading heads used in the fatigue machine. On the other flange the strains are very strongly affected by the proximity of the gages to a section where the concrete is cracked and also by the local effects of the load transmitted by the stud shear connector.

If the linear strain distribution recorded in the web is extrapolated to the flanges, the moment determined from this distribution is in almost complete agreement with that determined on the basis of statics for the beam structure. This would certainly seem to verify the fact that deviations from this distribution, as recorded by the strain gages, are caused by the local circumstances noted previously.

All beams in this series failed by propagation of a fatigue crack through the tension flange. These cracks initiated on the edge of the stud shear connectors, as in all previous tests conducted on beams and plate specimens. The fractures initiated at the row of studs just removed from the pure moment region of the beam span. This location agrees with that expected since between the support point and the point of load

application, the beam is subjected to a constant value of shear and a linear increase in bending moment. All studs in this region, therefore, are required to transmit the same shear force and the one row of studs nearest the point of maximum moment is the most likely point for any fatigue failure to initiate. Although the row of studs at midspan is subjected to a slightly higher moment, they are not subjected to any shear force and are, therefore, not the most critical.

On the basis of all beam tests conducted, it would appear that the fatigue resistance of beams with reinforced concrete cover is the same as that obtained from the plate tests. A comparison of the beam tests indicates that the presence of the reinforced concrete produces a condition which is slightly more severe than the plain beam but not quite as severe as when the studs are loaded by the mechanical flexors.

FRACTURE SURFACES

The fracture surfaces obtained in all fatigue tests followed the same pattern with the fracture initiating at or near the edge of the stud which is first encountered by the axial stress flow. Initial cracks occurred at either one of these locations or at both of them, more or less simultaneously. As the test progressed, one of the cracks, in those cases where two cracks initiated, propagated more rapidly and caused the other crack to stop propagating.

Typical fracture surfaces for the various specimens tested are shown in Figures 16 through 19. The general features of the fractures shown in Figure 16 are very similar and indicate the general nature of all fracture surfaces encountered in the test

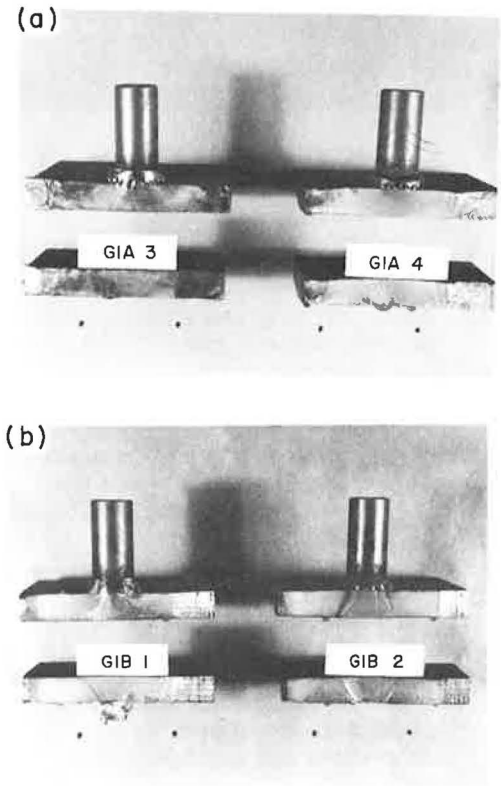

Figure 16. Typical fracture surfaces of single-stud specimens: (a) A7F steel, and (b) A441 steel.

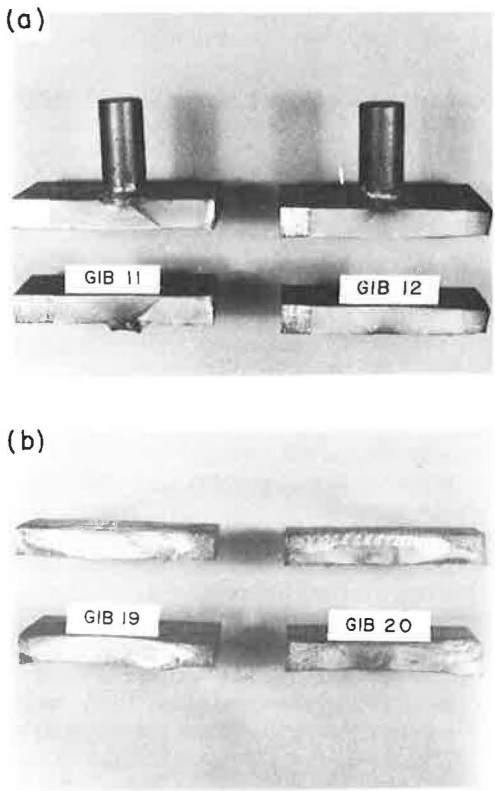

Figure 17. Fracture surfaces of specimens with altered geometry: (a) ground upset, and (b) stud completely removed.

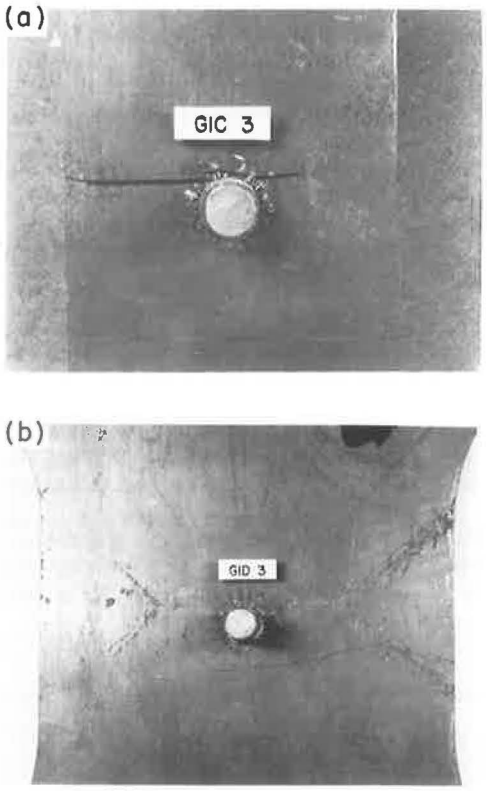

Figure 18. Fractures of single-stud wide-plate specimens: (a) 5 in. wide, and (b) 10 in. wide.

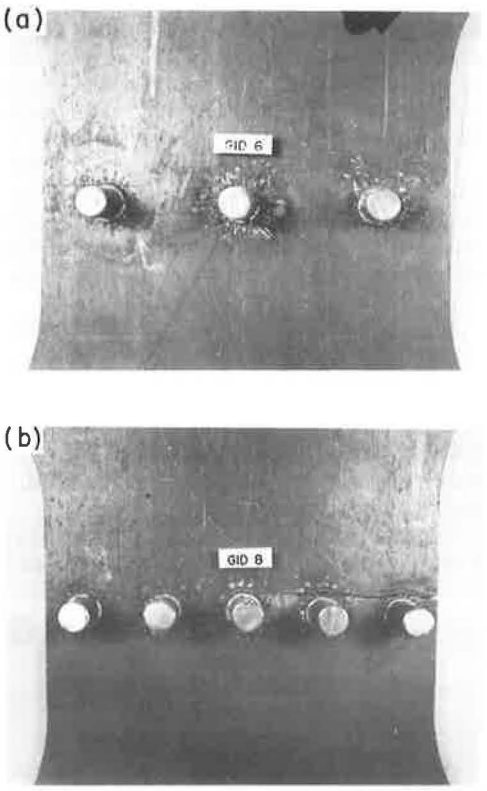

Figure 19. Fractures of multiple-stud wide-plate specimens: (a) three studs, and (b) five studs.

program. Typical features include a region generally referred to as the "thumbnail," where the rate of propagation is relatively slow. As the crack grows in size, the rate of propagation increases and the fracture surface is somewhat rougher. The final stage of fracture is a static failure of the remaining area of the test specimen.

Particular note should be taken of Figure 16b which shows the fracture surface for GIB1. In this specimen the fracture actually initiated under the upset. As the crack propagated, it cut across the upset as well as the parent plate, so that when final fracture occurred a portion of the upset was torn from around the stud. This type of failure was encountered in a few of the cases in this study and was primarily affected by the extent to which the upset was bonded to the parent plate. When the upset was not completely bonded, the critical location was actually under the upset and the fracture propagated from this point.

Figure 17 shows the fracture surfaces which resulted when the geometry of the upset was altered. The top portion of this figure shows the result when the upset was ground to a smooth transition between the parent plate and the stud. Failure surfaces in this case are very similar to those previously presented except that the region of slow propagation is somewhat larger than when the upset is subjected to no treatment. Figure 17b shows the fracture surfaces which resulted in the two cases where the stud was completely removed. Here again the fracture surface is not greatly different from that previously reported, except that the region of slow propagation is somewhat larger. The failures initiated at locations corresponding to where the edge of the stud would have been, had it not been removed. This would indicate that the metallurgical structure in this area is weaker as a result of the changes occurring during the welding

process. The fatigue test results indicate, however, that the influence of this metallurgical change is not nearly as great as the geometrical effect of the presence of the upset.

Figure 18 shows the fracture locations for the cases where a single stud was attached to a wider plate. The fracture surfaces in these cases were similar to those previously presented. A very interesting feature of the multiple stud specimens is shown in Figure 19, where typical failures of wide plates with multiple studs are presented. Close examination of the photograph of specimen GID6 reveals several independent cracks which have initiated in a manner identical to that obtained for the plate specimens with a single stud. The photograph of specimen GID8 shows how these cracks which initiate and propagate independently join up to form a continuous crack which eventually causes final fracture.

Although it is not readily apparent in the photographs of the specimens with multiple studs, close examination of the specimens revealed that a large number of independent cracks had actually initiated. In the case of the specimens with three studs, at least three independent cracks were initiated. In the case of the specimens with five studs, the number of independent cracks varied from six to eight, indicating that in all cases at least some cracks were initiated on both sides of the studs. This observation is of particular importance since it indicates that the fatigue resistance of such installations is not a case of the weakest link but rather that the fatigue resistance of all of the studs is virtually the same and that fracture initiates at all studs at very nearly the same number of cycles. Some further indication of this fact is contained in the following section.

METALLURGICAL STUDIES

As a part of the program it was essential that detailed metallurgical studies be carried out to determine the nature of the microstructure as influenced by base material, heat input and amount of material available to absorb the heat input during the welding process. A total of five different specimens was subjected to detailed examination. Most of these specimens were examined after completion of the fatigue test. In one case the specimen was subjected to metallurgical study in the as-produced condition to verify that at the examination section the fatigue loading had produced no change.

Both macro- and micrographs of areas of interest were taken for all specimens studied. The studies also included detailed hardness traverses from baseplate material to unaffected base-stud material, across the heat-affected zones and the weld-metal microstructure.

Microstructures

The general microstructural features of the stud welds are typical of welds in general: a columnar weld-metal zone, with ferrite outlining of the prior austenite matrix. This weld-metal zone is a mixture of tempered martensite, ferrite and pearlite at room temperature. The next portion of the microstructure is the heat-affected zone which possesses an austenite grain size gradient (largest grains near the fusion line), resulting in the presence of martensite near the fusion line. Away from the fusion line the amount of martensite decreases and the amount of pearlite and ferrite increases. Adjacent to this region is the unaffected base-metal zone which consists of Widmanstätten ferrite and pearlite in a banded structure due to the hot rolling process.

Detailed macro- and micrographs of a variety of specimens are contained in Figures 20 through 24. Hardness surveys from the baseplate material across the heat-affected zone and weld metal to the base material of the stud are contained in Figures 25 through 28. The specific microstructures vary somewhat in width of the heat-affected and weld-metal zones. The relative amount of martensite in the heat-affected and weld-metal zones and the fineness of the columnar structure of the weld metal vary as a result of the difference in the heat input to the various specimens. The amount of weld metal increases with the amount of heat input to the specimens, as does the width

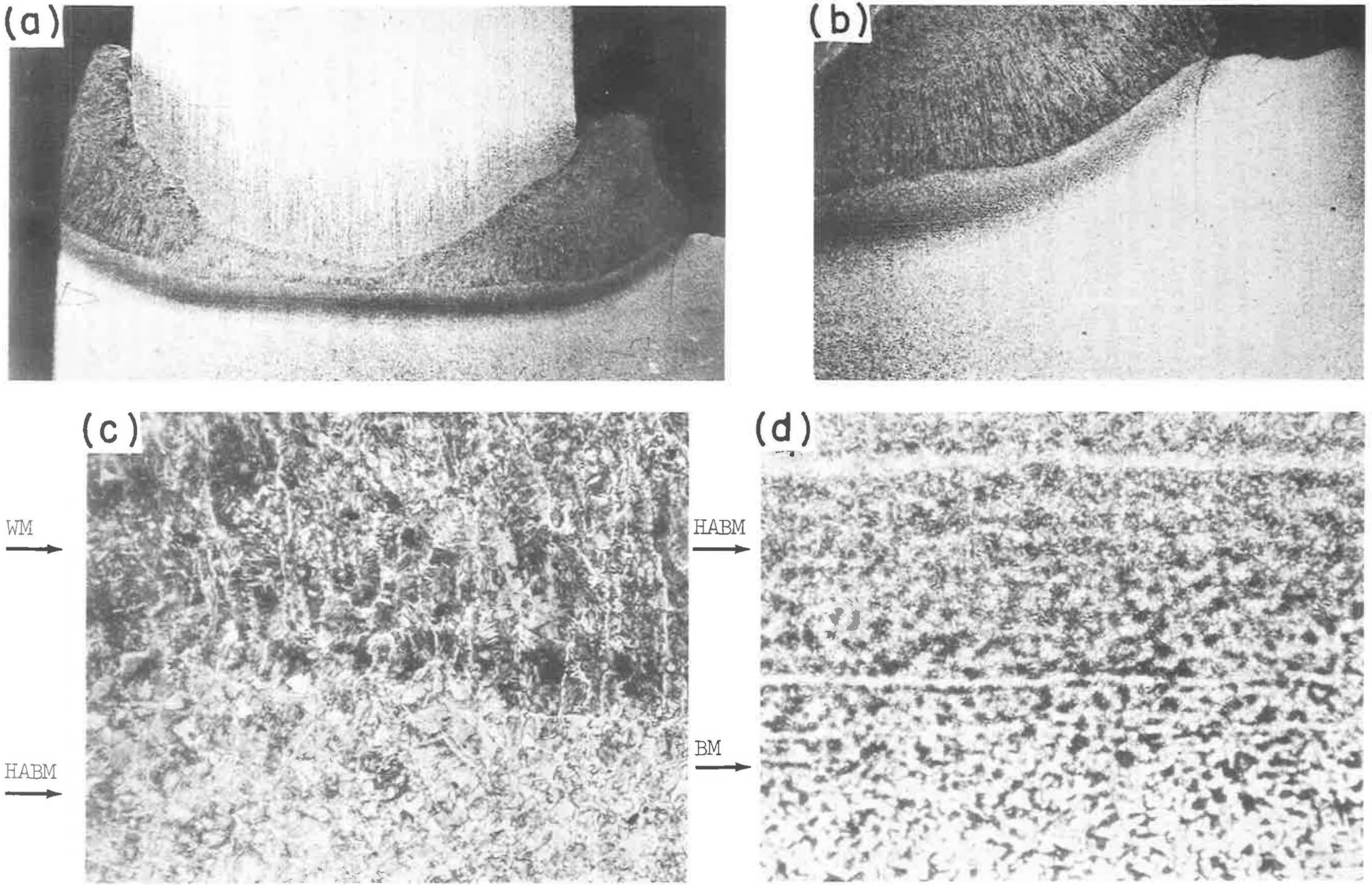

Figure 20. Specimen GIA2: (a) macrograph 3X; (b) macrograph 6X; (c) and (d) micrographs 72X.

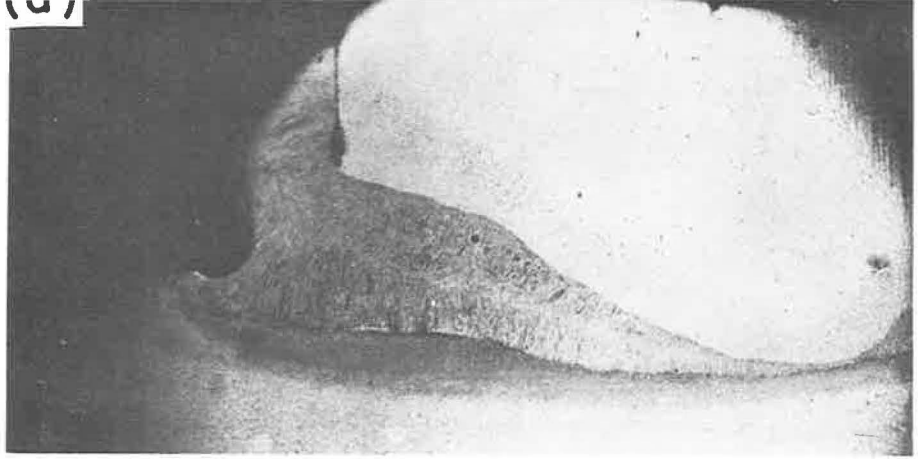

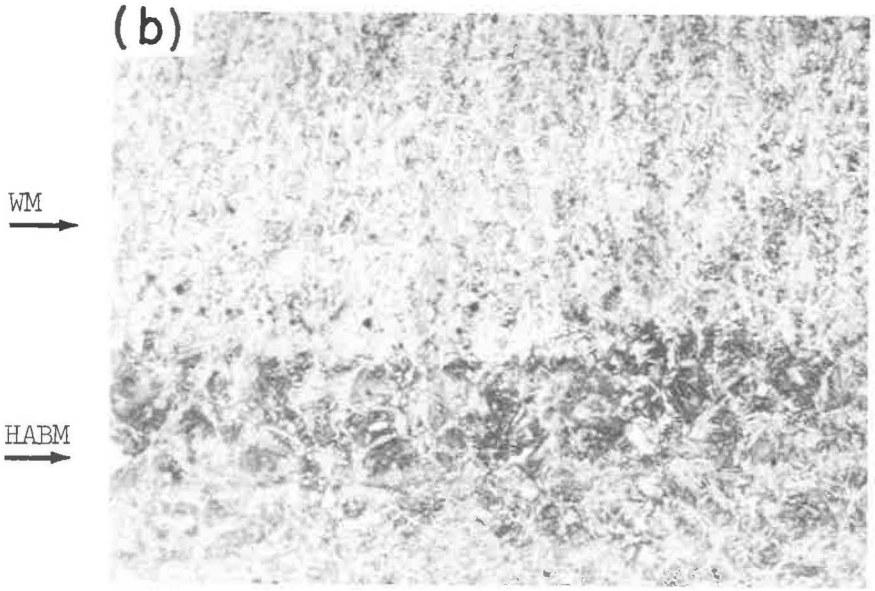

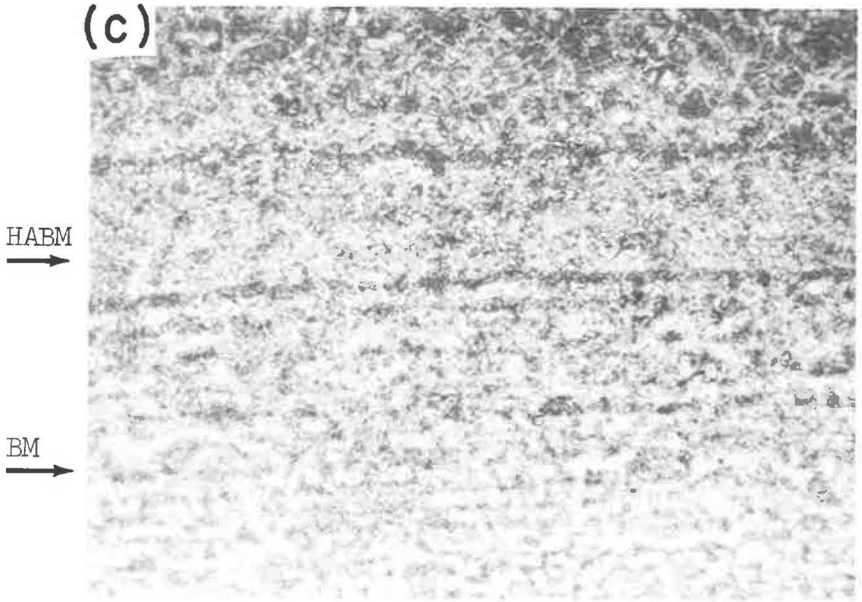

Figure 21. Specimen GIB1: (a) macrograph 5X; (b) and (c) micrographs 72X.

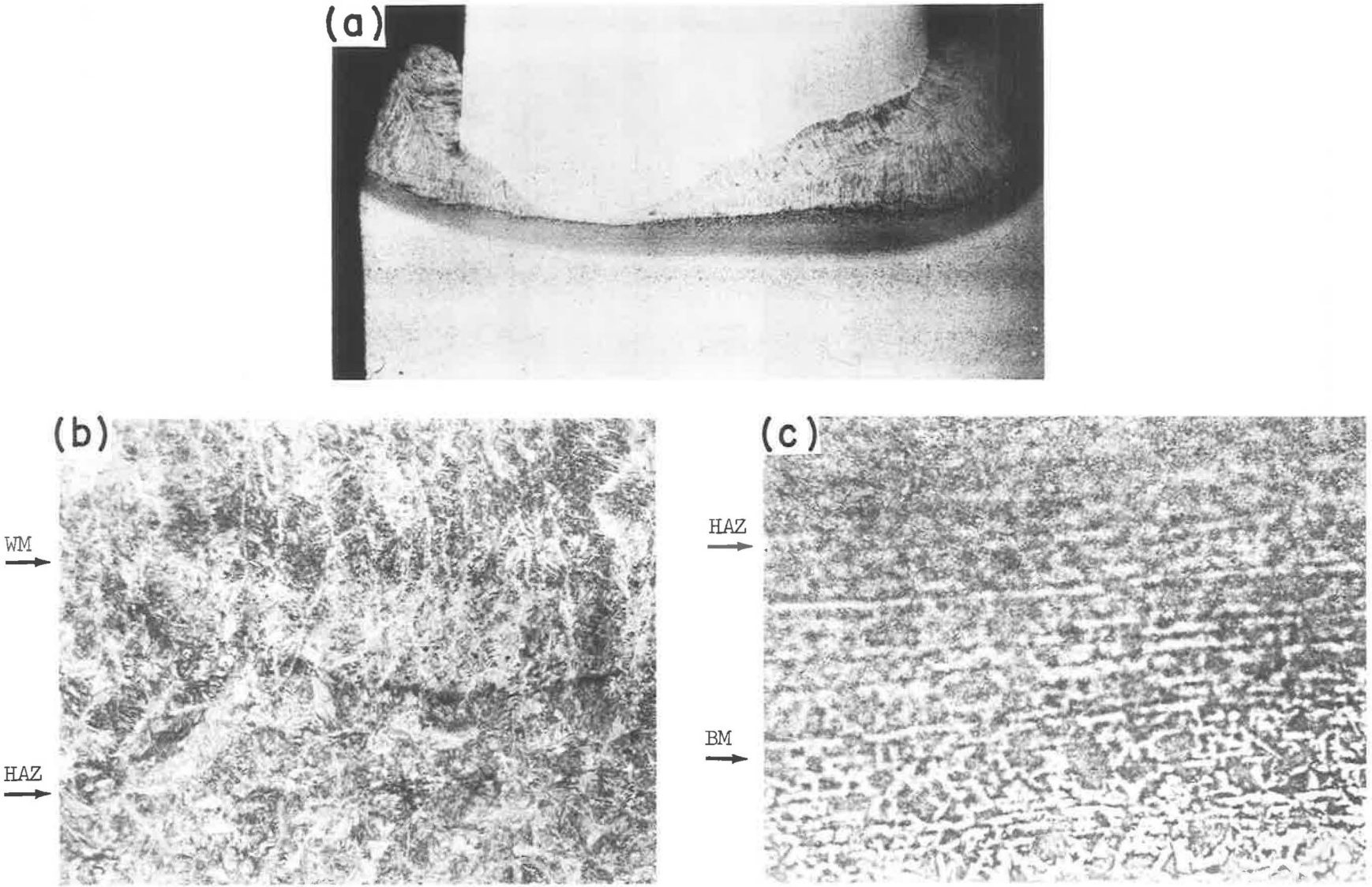

Figure 22. Specimen GIB16: (a) macrograph 3X; (b) and(c) micrographs 75X.

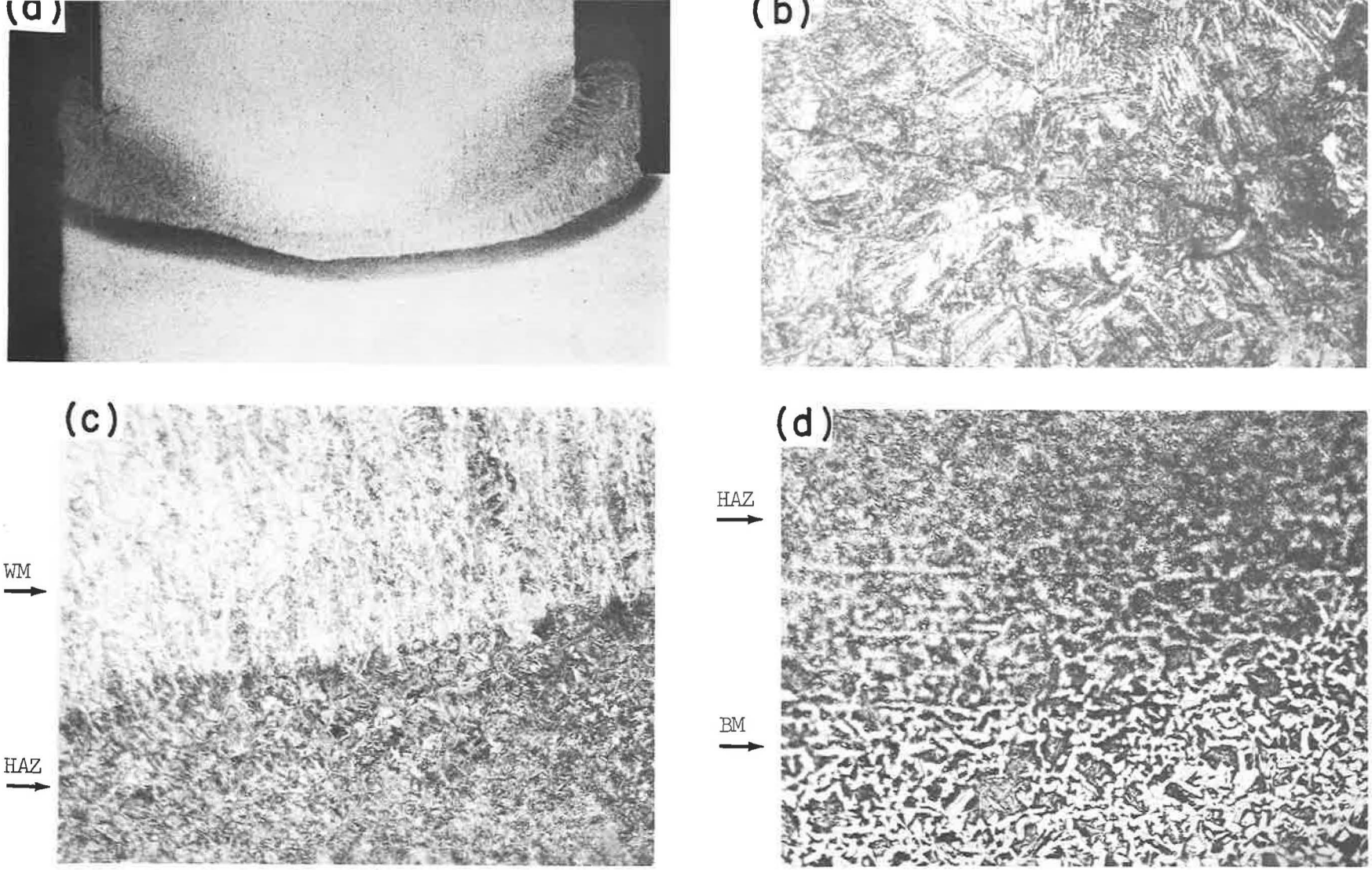

Figure 23. Specimen GIC2: (a) macrograph 3X; (b) micrograph 500X, showing crack in HAZ; (c) and (d) micrographs 75X.

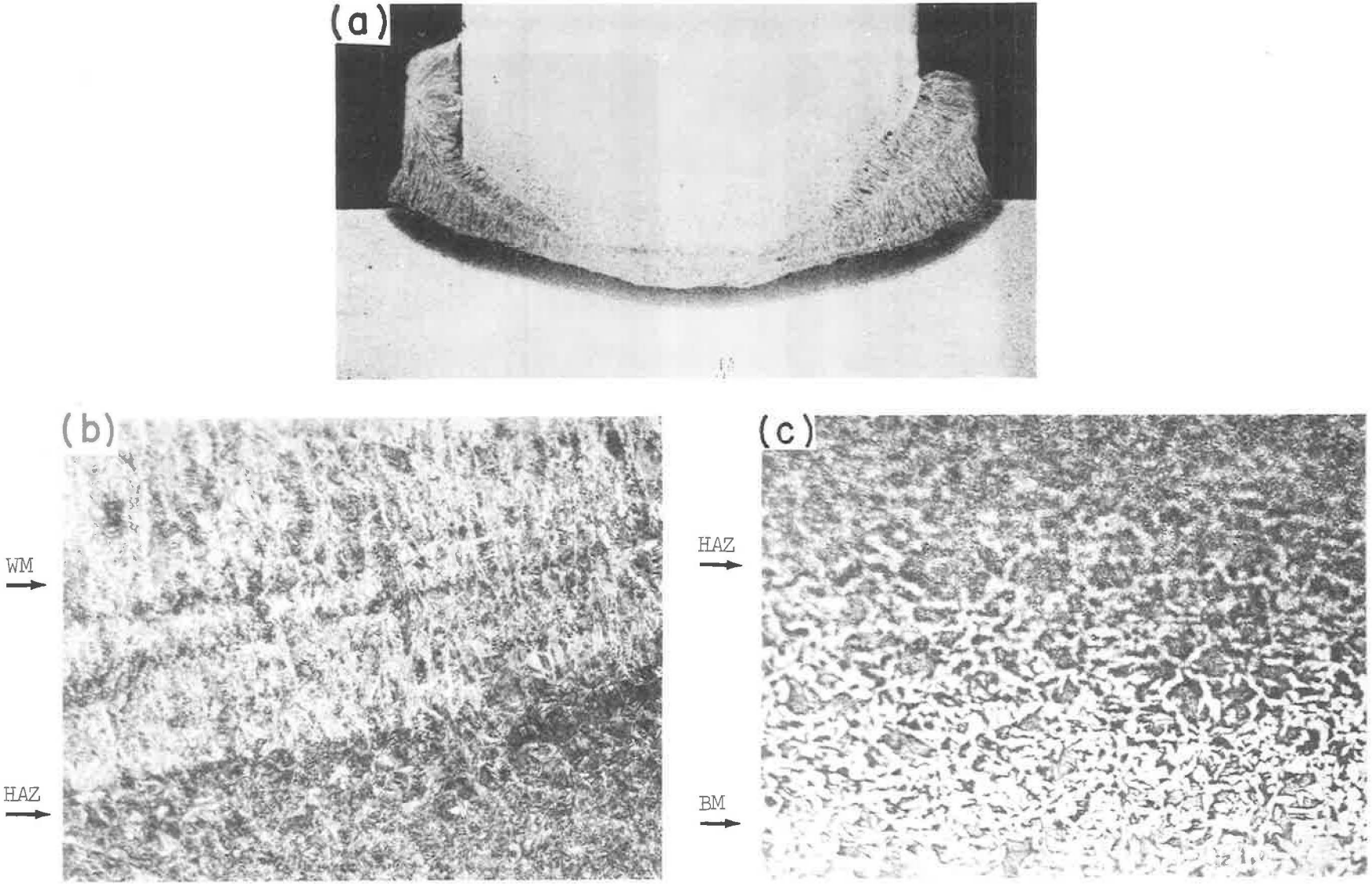

Figure 24. Specimen GIC5: (a) macrograph 5X; and (b) and (c) micrographs 75X.

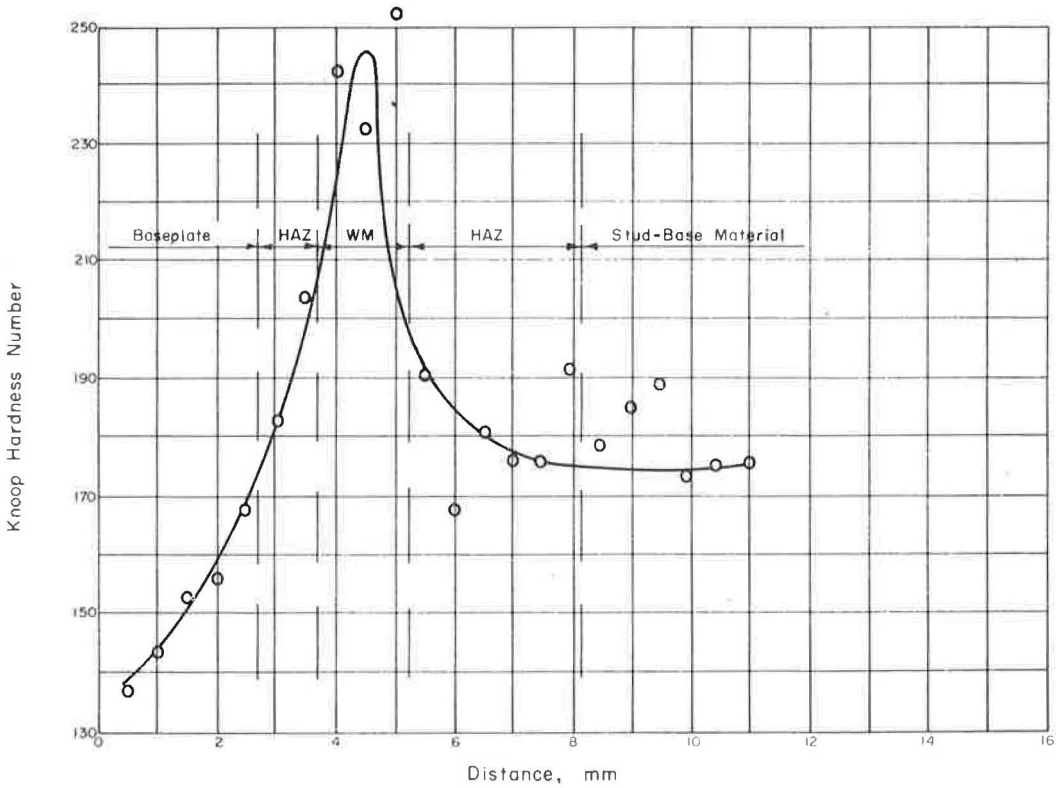

Figure 25. Hardness survey, specimen GIA2.

of the heat-affected zone. Consequently, GIA2 and GIC5 have the narrowest weld-metal and heat-affected zones, followed by GIB1 and GIB16, and the fineness of the weld-metal structure decreases in the same order. Specimen GIB16 has a higher percentage of martensite in the heat-affected zone than GIB1.

Although an increase in heat input generally decreases the hardenability, the opposite is true for this material. The presence of the strong carbide former, vanadium, ties up some carbon and long solution times are required to take the carbon back into solution. As a result, more carbon is in solution in GIB16 than in GIB1, which accounts for the increased amount of martensite. Specimen GIB1 would be expected to have a smaller amount of martensite than GIC5 due to the lower heat input, and GIA2 would have less martensite due to the decreased hardenability of A7F steel as compared to A441 steel. Since the weld metal is formed by melting the base metal, the same trends observed in the heat-affected zone should be observed in the weld-metal zones.

Hardness Surveys

As would be expected on the basis of metallographic observation, the hardness of the material increases as the percent of martensite increases. As a result, the hardness of the heat-affected zone of the plate GIB16 is considerably higher than that of GIB1, and the same is true of the weld-metal zones. It is also true that the hardness of the heat-affected zone of the plate and the weld-metal zone of GIB1 is considerably higher than the corresponding hardness in these regions of GIA2, due to the increased alloy content of A441 steel as compared to A7F. Table 10 contains a summary, from four different specimens, of the size and average hardness of the various zones which result from the welding operation.

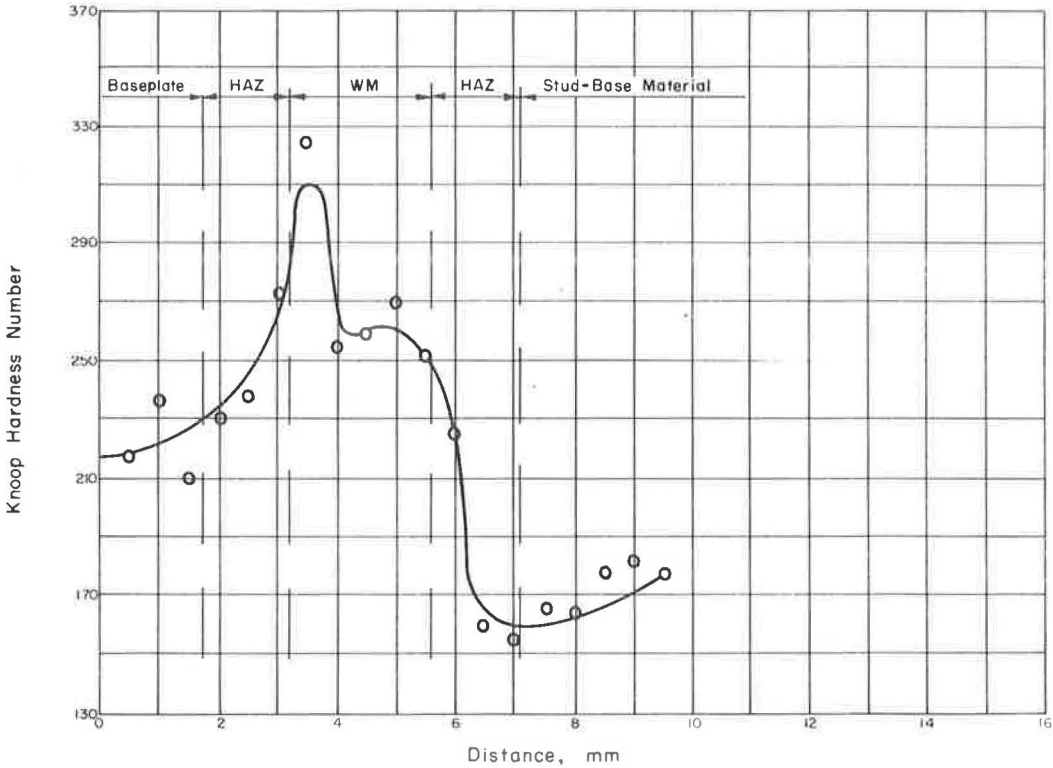

Figure 26. Hardness survey, specimen GIB1.

Mode of Failure

Typical failure of all specimens is evidenced in GIA2. Both of the macrographs in Figure 20 shows a fatigue crack on the right-hand edge of the stud which initiated at the fusion line and traversed the heat-affected zone. This is not the crack which resulted in final failure of the specimen but is rather 180° away from the source of ultimate failure. Propagation of the crack is transgranular as seen in GIA2.

SUMMARY

The tests reported give a very good indication of the effect of base material, number of stud connectors, spacing of stud connectors and welding procedure on the fatigue resistance. On the basis of the flat-plate test series, the following conclusions have been drawn:

1. In all cases, the fracture initiated at the edge of the upset and propagated radially through the thickness of the plate. Almost without exception the multi-studded specimens featured more than one independent fracture surface. All multiple fractures occurred almost simultaneously.
2. The stress range to produce failure in 2,000,000 cycles varied from 16,000 psi in complete reversal to 14,000 psi in a half tension-to-tension stress cycle.
3. There was no noticeable difference in fatigue life between specimens fabricated from A7F or A441 base material.
4. Altering the stud-welding procedure to supply more heat to the weld had no effect on the fatigue life.
5. Changing the stud geometry by grinding the upset to a smooth transition doubled the fatigue life. Complete removal of the studs provided an even greater resistance to

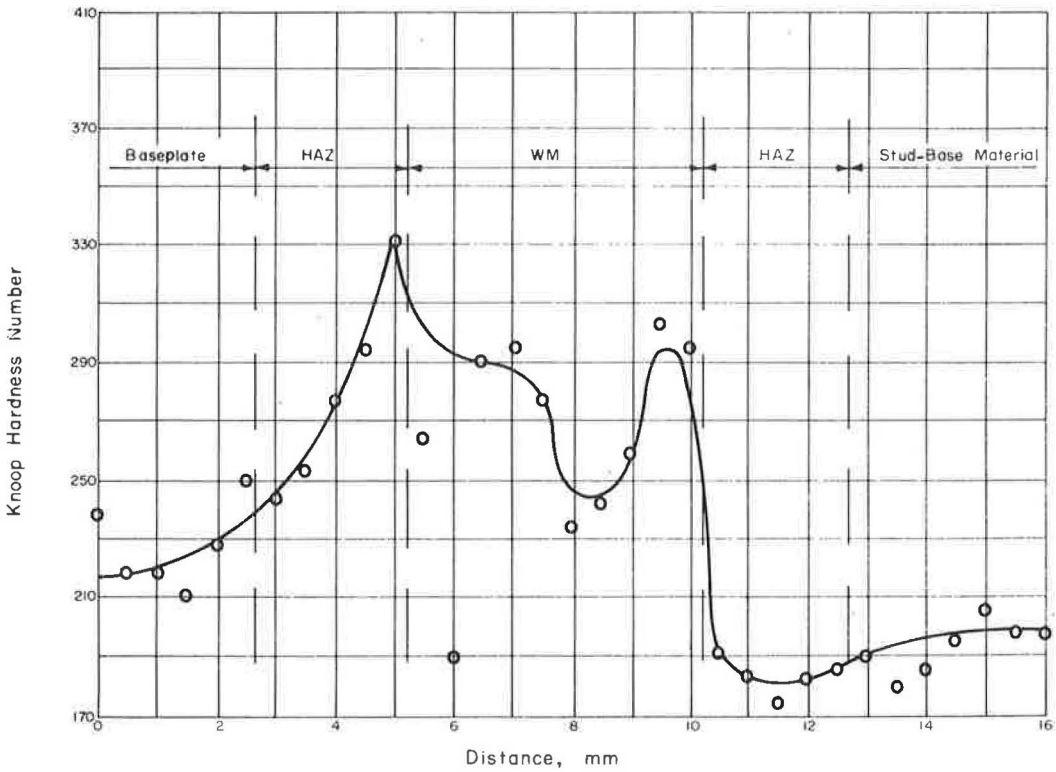

Figure 27. Hardness survey, specimen GIB16.

fatigue loading. With the stud removed, however, the fatigue life was not as great as has been reported earlier for plain-plate specimens of similar material.

6. The number of studs in a line transverse to the direction of stress and the spacing of the studs has some effect on the fatigue resistance but the effect is not very large.

The behavior of the beam specimens in all three series was very similar to what was obtained for the flat-plate specimens. Excellent correlation is obtained between the flat-plate specimens and the beam specimens, not only in overall behavior but also in terms of stress levels required to produce failure in 2,000,000 cycles. The following observations have been made on the basis of the beam tests:

1. Fractures in the beam specimens were similar to those obtained in the flat-plate specimens. In flat-plate specimens the fracture might occur on either side of the stud, whereas in the beam specimens, the fractures occurred on the side of the stud where secondary tensile stresses, due to the loading of the stud, were added to the primary tensile flexural stresses.

2. Cracking occurred in the concrete at every row of studs and only at the studs. Although the slab used in these tests was narrow, there is reason to believe that shear connectors in the negative moment regions might prove to be an effective means of crack control.

3. The half tension-to-tension stress cycle to produce failure in 2,000,000 cycles for the various groups of beams tested was plain beams, 16.4 to 32.8 ksi; beams with flexors, 12.5 to 25.0 ksi; and beams with concrete, 14.0 to 28.0 ksi. In view of the extent of the agreement between the results of the flat-plate and beam specimens, it would certainly appear that the flat-plate tests give a satisfactory indication of the behavior of similar beam tests.

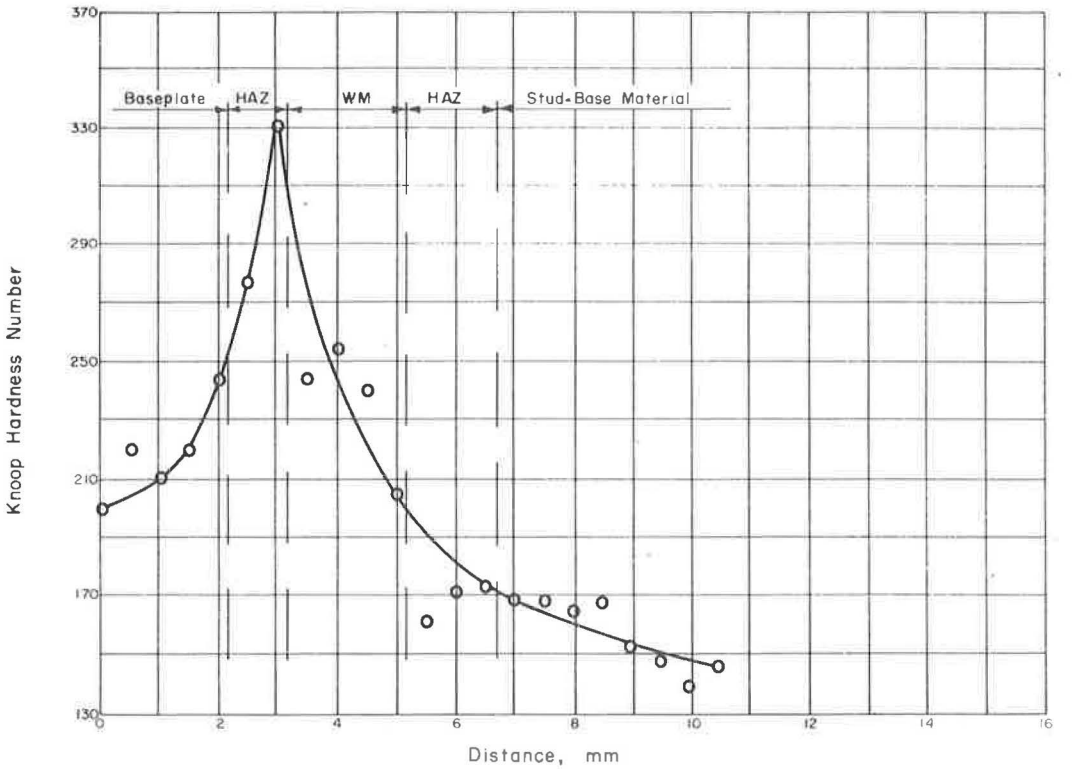

Figure 28. Hardness survey, specimen GIC5.

TABLE 10

EFFECT OF STUD-WELDING PROCEDURE

Item	Value			
Specimen	GIA2	GIB1	GIB16	GIC5
Type of steel	A7F	A441	A441	A441
Heat input[a]:				
Weld current (amp)	1,500	1,500	1,450	1,750
Arc voltage (volts)	33	33	33	31
Weld time (cycles)	58	58	76	43
Heat (KVA cycles)	2,870	2,870	3,630	2,330
Zone widths (mm):				
Heat-affected zone stud	3.0	1.5	2.5	1.5
Weld metal	1.5	2.5	5.0	2.0
Heat-affected zone plate	1.0	1.5	2.5	1.0
Avg. zone hardness (Knoop):				
Base metal stud	180	171	195	157
Heat-affected zone stud	181	179	184	169
Weld metal	143	255	266	237
Heat-affected zone plate	194	248	283	305
Base metal plate	150	222	228	215

[a]Lift of 3/32 in. and plunge of 3/16 in. used.

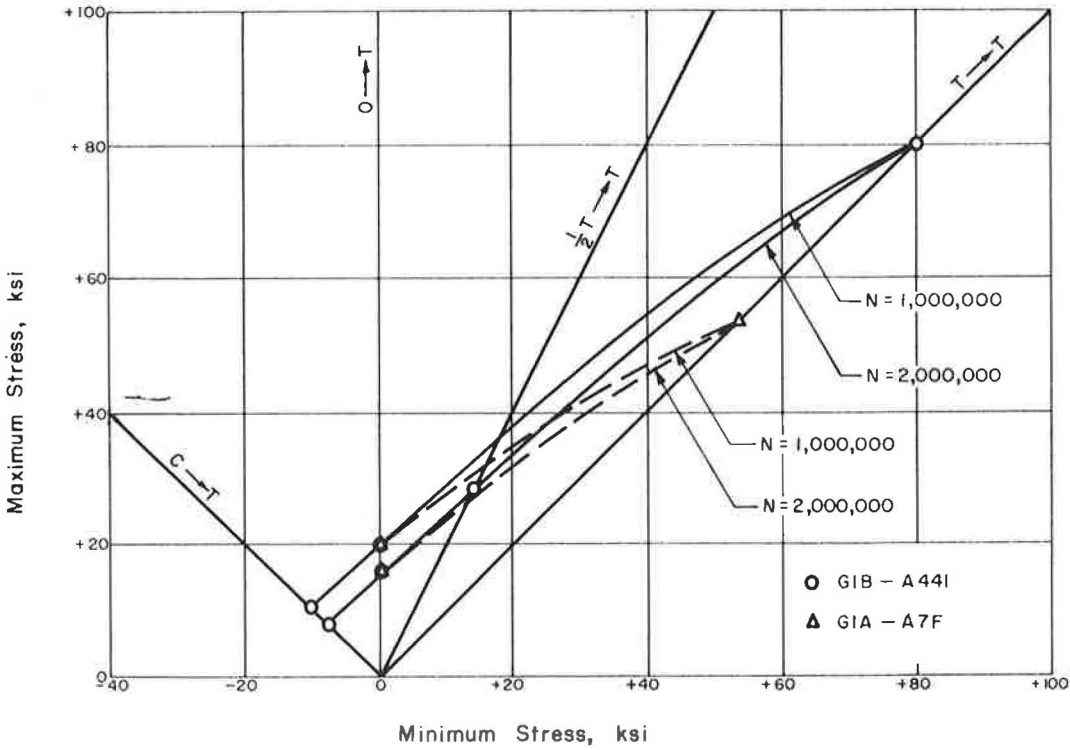

Figure 29. Modified Goodman diagram for GIA and GIB specimens.

With this as a basis, the modified Goodman diagram presented in Figure 29 should serve for the development of suitable provisions for fatigue in the case of designs which utilize stud shear connectors for composite action in negative moment regions. This diagram yields a stress range of 16,000 psi for complete reversal, 16,000 psi for zero-to-tension, and 14,000 psi for half tension-to-tension for failure in 2,000,000 cycles. A somewhat smaller range would be required for stress cycles above this level. Applying a factor of safety of approximately 1.6 on these stresses results in permissible stress cycles of approximately 10,000 psi.

ACKNOWLEDGMENTS

The tests described herein were conducted in the structural laboratories of the Civil Engineering Department at the University of Illinois under the sponsorship of Gregory Industries, Inc. The tests were conducted by K. A. Selby, at the time research assistant in Civil Engineering. The authors wish to express their appreciation to W. T. Becker, Research Assistant, who conducted the metallurgical studies, and the members of the Civil Engineering Shop who prepared the test members.

REFERENCES

1. Viest, I. M. Review of Research on Composite Steel Concrete Beams. Jour. ASCE, Vol. 86, No. ST6, June 1960.

2. Stallmeyer, J. E., Nordmark, G. E., Munse, W. H., and Newmark, N. M. Fatigue Strength of Welds in Low-Alloy Structural Steel. Suppl. to Welding Jour., June 1956.
3. Wilson, W. M., and Thomas, F. P. Fatigue Tests of Riveted Joints. Univ. of Illinois Eng. Exper. Sta. Bull. 302, 1938.